Gene therapy to the blood-brain barrier with resulting protein secretion as a strategy for treatment of Niemann Picks type C2 disease

Hede, Eva; Christiansen, Christine Bodelund; Heegaard, Christian Würtz; Moos, Torben; Burkhart, Annette

Published in:
Journal of Neurochemistry

DOI (link to publication from Publisher):
10.1111/jnc.14982

Publication date:
2021

Document Version
Accepted author manuscript, peer reviewed version

DR. ANNETTE BURKHART (Orcid ID : 0000-0003-2086-4693)

Article type : Original Article

Gene therapy to the blood-brain barrier with resulting protein secretion as a strategy for treatment of Niemann Picks type C2 disease

Eva Hede[1], Christine Bodelund Christiansen[1], Christian Würtz Heegaard[2], Torben Moos[1], Annette Burkhart[1]*

[1] Laboratory of Neurobiology, Biomedicine Group, Department of Health Science and Technology, Aalborg University, 9220 Aalborg, Denmark

[2] Department of Molecular Biology and Genetics - Molecular Nutrition, Aarhus University, 8000 Aarhus C, Denmark

*** Correspondence:**
Annette Burkhart
Laboratory of Neurobiology, Biomedicine Group
Department of Health Science and Technology
Fr. Bajers Vej 3B, 2.104,
Aalborg University, DK-9220 Aalborg East, Denmark,
Phone: + 45-99442420
E-mail: abl@hst.aau.dk

Running title: Gene therapy to rat brain endothelial cells as a strategy for treatment of Niemann Picks type C2 disease

Abbreviations:

BBB, blood-brain barrier; **BCECs,** brain capillary endothelial cells; **bNPC2**, bovine Niemann Picks disease type C2 protein; **BSA**, bovine serum albumin; **CTP-cAMP**, 8-(4-Chlorophenylthio)adenosine 3′,5′-cyclic

monophosphate sodium salt; **CLD5**, Claudin 5; **CNS**, central nervous system; **DAPI**, 4′,6-diamidino-2-phenylindole dihydrochloride; **DMEM**, Dulbecco's Modified Eagle Medium; **DMSO**, dimethyl sulfoxide; **ELISA**, Enzyme-Linked Immunosorbent Assay; **FCS**, Fetal Calf serum; **HC**, Hydrocortisone; **LSD**, Lysosomal storage disease; **MPR300**, Mannose-6-phosphate receptor (Cation independent); **M6P**, Mannose-6-phosphate; **NPC2**, Niemann Picks disease type C2 protein; **OCLN**, Occludin; **OFP**, Orange fluorescent protein; **Papp**, apparent permeability; **PBS**, phosphate-buffered saline; **PDS**, Plasma-derived bovine serum; **rBCECs**, rat brain capillary endothelial cells; **RO**, 4-(3-Butoxy-4-methoxybenzyl)-2-imidazolidinone; **TEER**, trans-endothelial electrical resistance; **TMB**, Tetramethylbenzidine; **WT**, Wild type; **ZO1 and ZO2,** zonula occludens 1 and 2.

Keywords: Blood-brain barrier, gene therapy, primary culture, Niemann Picks disease type C2, Cholesterol, NPC2 deficient fibroblasts

ABSTRACT

Treatment of many diseases affecting the central nervous system (CNS) is complicated by the inability of several therapeutics to cross the blood-brain barrier (BBB). Genetically modifying brain capillary endothelial cells (BCECs) denotes an approach to overcome the limitations of the BBB by turning BCECs into recombinant protein factories. This will result in protein secretion towards both the brain and peripheral circulation, which is particularly relevant in genetic diseases, like lysosomal storage diseases (LSD), where cells are ubiquitously affected both in the CNS and the periphery. Here we investigated transfection of primary rat brain capillary endothelial cells (rBCECs) for synthesis and secretion of recombinant NPC2, the protein deficient in the lysosomal cholesterol storage disease Niemann-Pick type C2. We demonstrate prominent NPC2 gene induction and protein secretion in 21 % of BCECs in non-mitotic monocultures with a biological effect on NPC2 deficient fibroblasts as verified from changes in filipin III staining of cholesterol deposits. By comparison the transfection efficiency was 75 % in HeLa-cells, known to persist in a mitotic state. When co-cultured with primary rat astrocytes in conditions with maintained BBB properties 7 % BCECs were transfected, clearly suggesting that induction of BBB properties with polarized conditions of the non-mitotic BCECs influences the transfection efficacy and secretion directionality. In conclusion, non-viral gene therapy to rBCECs leads to protein secretion and signifies a method for NPC2 to target cells inside the CNS otherwise inaccessible due to the presence of the BBB. However, obtaining high transfection efficiencies is crucial in order to achieve sufficient therapeutic effects.

INTRODUCTION

The restrictive functions of the blood-brain-barrier (BBB) constitute a major hurdle in the development of new therapies for diseases affecting the central nervous (CNS) such as neurodegenerative disorders, neurovascular diseases, neurological infections, and CNS tumors (Pardridge 2005). In close contact with pericytes and astrocytic end-feet, the BBB is composed of brain capillary endothelial cells (BCECs), which comprise a physical and biological barrier, separating the CNS from the circulation. The BBB is crucial for the maintenance of a stable microenvironment within the CNS including protection from entry of potentially harmful substances, which is essential for ideal neuronal function (Daneman *et al.* 2010; Abbott *et al.* 2009; Alvarez *et al.* 2011; Misje Mathiisen *et al.* 2010; Armulik *et al.* 2010). Numerous different approaches have been investigated with the aim of overcoming this hurdle, including direct infusion into the BBB, temporarily opening of the BBB, and exploiting existing BBB transport mechanisms. However, these are often associated with a risk of severe adverse events, lack of specificity or poor distribution within the CNS (Assmann *et al.* 2016; Tajes *et al.* 2014; Johnsen *et al.* 2017; Johnsen and Moos 2016).

Instead of trying to overcome the limitations of BBB, another strategy uses the BBB as a target for drug delivery by genetically modifying the BCECs to produce and secrete therapeutic molecules to the brain (Burkhart *et al.* 2017; Jiang *et al.* 2003; Thomsen *et al.* 2011; Chen *et al.* 2009). As the neurons within the CNS are rarely located more than 8-20 μm from the capillaries, molecules secreted by the BCECs will be available throughout the entire brain with a minimum need for passive diffusion through the extracellular space (Abbott *et al.* 2006). Genetically modifying the BCECs thus represents a novel and promising strategy for drug delivery to the CNS (Déglon and Hantraye 2005). However, this strategy is very dependent on the use of an ideal vector for gene delivery. Both viral and non-viral vectors have been studied comprehensively throughout the years and while viral vectors are still generally considered to induce the highest level of gene modification, non-viral vectors are generally considered safer to use, due to a lower risk of immunological and pathogenic reactions (Choong *et al.* 2016; Simonato *et al.* 2013). We have previously shown that non-viral gene therapy can induce secretion of growth hormone and erythropoietin from BCECs in the direction of both the blood and the brain (Thomsen *et al.* 2011; Burkhart *et al.* 2017). While secretion towards the blood side of the BBB could involve a serious risk of adverse events in diseases solely affecting the CNS, it has the potential for delivery of protein to all cells in the body, including the CNS, which is especially relevant in diseases involving a global protein deficiency. This is the case in a number of rare genetic metabolic diseases like the lysosomal storage diseases (LSD), which are characterized by lysosomal dysfunctions due to either enzymatic or non-enzymatic protein deficiencies (Ashtari *et al.* 2016).

Niemann-Pick type C (NPC) disease denotes a specific LSD in which the lysosomal dysfunction is caused by a deficiency in either of two lysosomal cholesterol transporters, NPC1 or NPC2 (Ashtari *et al.* 2016; Vanier and Millat 2004; Storch and Xu 2009). It is a rare autosomal recessive disease with a clinical incidence of approximately 1:100,000 of which mutations in the NPC2 gene comprises 5% of the cases, while 95 % of the cases are caused by mutations in the NPC1 gene (Vanier 2010). However, the disease is believed to be significantly underdiagnosed due to a lack of clinical awareness (Vanier 2010). It is a severe disease with a broad variety of both systemic and CNS symptoms, which results in premature death in almost all cases (Vanier 2010). About 10 % of the patients die before six months of age, while others live for years, but rarely survive beyond 30 years of age (Vanier and Millat 2003; Wraith *et al.* 2009). Currently, the treatment options for these patients are mainly symptomatic (Vanier 2010). The only specific treatment, approved for this disease, is the glucosylceramide synthase inhibitor, Miglustat, which is able to delay the onset of symptoms and thereby increase survival but still without curing the disease (Vanier 2010; Patterson and Walkley 2017). While the NPC1 gene results in a large protein situated in the membranes of the lysosomes, the NPC2 gene encodes a small soluble protein, which can be both secreted and taken up by adjacent cells via the mannose-6-phosphate receptor (MPR300) (Fig. 7) (Storch and Xu 2009; Sands and Davidson 2006), making Niemann Picks type C2 disease an interesting candidate for gene therapy at the BBB. In other lysosomal storage disorders, this ability of cells to take up extracellular lysosomal enzymes and subsequently transport these to the lysosomes has been used for enzyme replacement therapies with varying outcomes (Beck 2009; Lim-Melia and Kronn 2009; Rohrbach and Clarke 2007; Fratantoni *et al.* 1968). Nevertheless, this approach has also been tested in a mouse model of Niemann-Picks disease type C2, where systemic injection of bovine NPC2 (bNPC2) protein, induced several visceral improvements (Nielsen *et al.* 2011). However, no significant improvements in neurological symptoms were observed following the systemic protein injections, indicating an inability for NPC2 to cross the BBB (Nielsen *et al.* 2011).

In this study, we aim at evaluating the potential of our previously proposed strategy of using gene therapy at the BBB to induce protein secretion to the CNS (Burkhart *et al.* 2017) by genetically modifying the BCECs to produce and secrete NPC2. Furthermore, we investigate the effect of recombinant NPC2 secreted from genetically modified cells on NPC2 deficient fibroblasts from a heterozygous NPC2 patient.

MATERIALS AND METHODS

The following reagents were purchased from Merck KGaA (Darmstadt, Germany, DE): Insulin transferrin sodium selenite (Cat. No. 11074547001), puromycin (Cat. No. P8833), collagen type IV (Cat. No. C5533), fibronectin (Cat. No. F1141), poly-L-lysine (Cat. No. P6282), hydrocortisone (HC) (Cat. No. H4001), Dimethyl Sulfoxide (DMSO) (Cat. No. D2650), 8-(4-Chlorophenylthio)adenosine 3′,5′-cyclic monophosphate sodium salt (CTP-cAMP) (Cat. No. C3912), 4-(3-Butoxy-4-methoxybenzyl)imidazolidin-2-one (RO) (Cat. No. B8279), 3,3',5,5'-Tetramethylbenzidine (TMB) (Cat. No. 860336), Hydrogen peroxide solution (Cat. No. 88597), Paraformaldehyde (Cat.No. 441244), Triton™-X-100 (Cat. No. X100), 4′,6-Diamidino-2-phenylindole dihydrochloride (DAPI) (Cat. No. D9542), Filipin III from *Streptomyces filipinensis (*Cat. No. F4767), TWEEN® 20 (Cat. No. P1379), and Poly(ethylene glycol) (Cat. No. 81260). The following reagents were purchased from Life Technology (Naerum, Denmark, DK): Fetal calf serum (FCS) (Cat. No. 10270), Dulbecco's Modified Eagle Medium consisting of nutrient Mixture F-12 (DMEM/F-12) (Cat. No. 31331), DMEM (low glucose) (Cat. No. 21885), DMEM (high glucose) (Cat. No. 31966), Trypsin (Cat. No 15090-46), and phosphate-buffered saline (PBS) (Cat. No SH3025802). Greiner bio-one Thincert cell culture insert for 12 well plates, with a transparent polyethylene terephthalate (PET) membrane and a pore diameter of 1 µm (Cat No. 665610) were purchased from In Vitro (Fredensborg, Denmark, DK). Basic fibroblast growth factor (Cat. No. 100-18B) was purchased from PeproTech Nordic (Stockholm, Sweden, SE). Gentamicin Sulfate (Cat.No. 17-518Z) was purchased from Lonza Copenhagen (Vallensbaek Strand, Denmark, DK). Plasma-derived bovine serum (PDS) (Cat. No. 60-00-810) was purchased from First Link (Wolverhampton, United Kingdom, UK). Bovine serum albumin (BSA) (Cat. No. EQBAH62) was purchased from Europa Bioproducts (Cambridge, United Kingdom, UK). Fluorescence mounting media (Cat. No S3023) was purchased from DAKO (Glostrup, Denmark, DK). GelRed™ Nucleic Acid Gel Stain (Cat. No. 41008) was purchased from VWR (Søborg, Denmark, DK). CytoFLEX Daily QC Fluorospheres (Cat. No. B53230) was purchased from Beckman Coulter (Copenhagen, Denmark, DK).

The following antibodies were purchased from Merck KGaA (Darmstadt, Germany, DE): Rabbit anti-Claudin 5 (CLD5) antibody (Cat no SAB4502981), mouse anti-vimentin antibody, clone V9 (Cat. No. MAB3400), rabbit anti-occludin (OCLN) antibody (Cat. No. ABT 146). The following antibodies were purchased from Life Technology (Naerum, Denmark, DK): Rabbit anti-zonula occludens 1 (ZO1) (Cat. No. 61-7300), rabbit anti-zonula occludens 2 (ZO2) (Cat. No.71-1400), Alexa Fluor 488-conjugated goat anti-rabbit IgG (Cat. No. A11034), Alexa Fluor 594-conjugated goat anti-rabbit IgG (Cat. No. A11037), and Alexa Fluor 488-conjugated donkey anti-mouse IgG (Cat. No. A21202). Mouse anti-NPC2 (D3) antibody (Cat No. sc166449, Santa Cruz Biotechnology) was purchased from AH Diagnostics (Aarhus, Denmark, DK). Rabbit anti-NPC2 antibody (Cat. No. TA332678) was purchased from Origene. Rabbit anti-MPR300

(Cation independent) antibody (Cat. No. AB32815) was purchased from Abcam. Human NPC2 ELISA pair set (Cat. No. SEK13341) from Sino Biological Inc. was purchased from Nordic BioSite (Copenhagen, Denmark, DK).

Human NPC2 Gene ORF cDNA clone expressing plasmid, C-OFPSpark tag (Cat. No. HG13341ACR) from Sino Biological Inc. was purchased from Nordic BioSite (Copenhagen, Denmark, DK). Lipofectamine 3000™ (Cat. No. L3000) and GeneJet plasmid Midiprep kit (Cat. No. K0481) were purchased from Life Technology (Naerum, Denmark, DK). Macherey–Nagel NucleoBond Xtra Midi EF plasmid DNA purification kit (#740420.50) was purchased from AH Diagnostics (Aarhus, Denmark, DK). Competent CG5 Escherichia coli strain (Cat. No. G3169) were purchased from Merck KGaA (Darmstadt, Germany, DE). 3H D-Mannitol (Cat. No NET101250UC) and Ultima Gold™ liquid scintillation cocktail (Cat. No. 6013326) were from PerkinElmer (Skovlunde, Denmark, DK).

Cell cultures

Primary cultures of rat brain capillary endothelial cells (rBCECs) were obtained from two to three week old Sprague Dawley rats (a mixture of female and male) as described previously (Burkhart *et al.* 2015b; Burkhart *et al.* 2015a). All procedures and handling of rats were approved by the Danish National Council for Animal Welfare (License no. 2013-15-2934-00893). Rats used in the experiment were obtained from in-house breeding while adult rats used for breeding were purchased from Javier labs. The pups were caged together with their mother until used in the experiment and all animals had unrestricted access to food and water and were housed under temperate conditions on a 12-hour light/dark cycle. All animals were sacrificed by decapitation between 8-9 am. Before decapitation of the rats, they were deeply anesthetized using isoflurane to avoid unnecessary interventions, and a total number of 18 rats were used for these experiments corresponding to two isolations of primary rBCECs. Isolated rBCECs were either cultured directly after isolation or frozen as capillaries for later use (FCS supplemented with 10% DMSO). All surface areas for culturing rBCECs were coated twice with collagen IV and fibronectin. rBCECs were maintained in rBCECs media consisting of DMEM-F12 supplemented with 10% PDS, 10 µg/ml Insulin transferrin sodium selenite, 1ng/µl basic fibroblast growth factor and 10µg/ml gentamicin sulfate. Puromycin (4µg/ml) was added to the rBCECs media for the first three days of culturing to remove potential contamination by pericytes (Perrière *et al.* 2005; Calabria *et al.* 2006), and rBCECs were not used for co-culture experiments with primary astrocytes until three days after isolation.

Primary astrocytes were obtained from two to three days old Sprague Dawley rats as described previously (Burkhart *et al.* 2015b). Astrocytes were maintained in astrocyte media consisting of DMEM (low Glucose) supplemented with 10% FCS and 10µg/ml gentamicin sulfate and all surface areas for astrocytes were

coated with poly-L-lysine. Astrocytes were cultured for a minimum of two weeks in T75 flasks before being frozen (astrocyte media supplemented with 20% FCS (30 % in total) and 7.5 % DMSO) for later use or seeded directly in 12 well plates at a density of 30,000 cells/cm^2 for co-culture experiments. Prior to co-culturing with rBCECs, the astrocytes were cultured for additionally two weeks without passaging to ensure a completely confluent monolayer of astrocytes.

To co-culture rBCECs with astrocytes, rBCECs were seeded at a density of approximately 100,000 cells/cm^2 on hanging culture inserts and left to adhere to the filter to obtain a confluent monolayer the following day. Induction of tight junctions and barrier integrity in the rBCECs was stimulated by moving the hanging filter insert containing rBCECs to the 12-well plate containing astrocytes and by the addition of CTP-cAMP (250µM), RO (17.5µM) and HC (550nM) to the media in the upper chamber and HC (550nM) to the media of the lower chamber. The media composition in the upper chamber were rBCECs media, while the lower chamber was a combination of rBCECs media and astrocyte conditioned media (1:1).

rBCEC were additionally seeded in collagen/fibronectin-coated 24 well plates at a cell density of approximately 100,000 cells/cm^2 to ensure a 100% confluent monolayer, and hereafter referred to as monocultures. All primary cells were used at passage P#1

The cervix cancer cell line HeLa (maximum passage number used P#15 after purchase from ATCC) was used as a positive control for transfection and protein secretion, as this cell line is easily transfected (Burkhart *et al.* 2017). HeLa cells were cultured in uncoated 24 wells plates and maintained in astrocyte media. HeLa cells were seeded at a cell density of 15,000 cells/cm^2 two days prior to experiments to ensure an 80-90% confluent monolayer.

Wild type (WT) human skin fibroblasts (GM08680) (maximum passage number used P#6) and NPC2 deficient human skin fibroblasts cell line (GM18455) (maximum passage number used P#10) (Nielsen *et al.* 2011) were maintained in DMEM (high glucose) supplemented with 10% FCS and 10µg/ml gentamicin sulfate. The NPC2 deficient human skin fibroblast cell line (GM18455) contains a missense mutation on one allele changing residue Cys-28 to Phe resulting in a disrupted di-sulfate bridge causing NPC2 to misfold. The other allele contains a nonsense mutation changing the residue Glu-1 to a stop codon, resulting in a truncated protein. Both fibroblast cell lines were seeded in uncoated 24 well plates at a density of 6,000 cells/cm^2.

None of the cell lines used are listed as a commonly misidentified cell line by the International Cell Line Authentication Committee and no further authentication, besides immunolabeling for cell-specific markers, was performed in the laboratory.

Transfection assay

Transfection was performed on rBCECs in co-culture with astrocytes, rBCECs in monoculture, monocultures of HeLa cells, and monocultures of NPC2 deficient fibroblasts. The cells were transfected to express the human version of the NPC2 gene using a pCMV3-C-OFPSpark plasmid. The plasmid was propagated in competent CG5 Escherichia E-Coli strain by heat shock transformation and the plasmid DNA was purified using the NucleoBond Xtra Midi EF plasmid DNA purification kit following manufactures instruction.

All cells were transfected using Lipofectamine 3000™. Prior to transfection, all cells received fresh media. The media used for rBCECs (both mono and co-culture) was changed to contain FCS instead of PDS. The following transfection protocol applies to a single 12 well-hanging filter insert or a single well in a 24 well plate both containing 750µl media. In one tube 0.5µg plasmid DNA was diluted in 25µl DMEM-F12 (rBCECs), DMEM low glucose (HeLa) or DMEM high glucose (Fibroblasts) together with the P3000 reagent (2µl/µg DNA). In another tube, 0.75µl Lipofectamine 3000™ was diluted in 25µl DMEM-F12 (rBCECs), DMEM low glucose (HeLa) or DMEM high glucose (Fibroblasts). Both solutions were mixed well and left to incubate at room temperature for 5 min before the Lipofectamine 3000™ solution was added to the diluted DNA. The combined mixture was mixed well and incubated at room temperature for 15 min for DNA:Lipofectamine 3000™ complexes to form. The DNA: Lipofectamine 3000™ complexes were added to the cells for 24 hours (rBCECs and HeLa) or 48 hours (Fibroblasts). At the end of the transfection period, the media was collected and stored at -80°C for later use (ELISA and NPC2 replacement assay) and the transfected cells were used either for flow cytometry or immunocytochemistry.

Evaluation of barrier integrity

To evaluate whether transfection of the rBCECs in co-culture had any effect on the barrier integrity of the rBCECs cell layer, both the trans-endothelial electrical resistance (TEER) and the passive permeability of Mannitol (182 Da) were determined. TEER was measured, using a MiliCell ERS-2 epithelial volt-ohm Meter and a STX01 chopstick electrode (Millipore, Hellerup, Denmark, DK). TEER was calculated by subtracting TEER values of double-coated but cell-free hanging filter inserts from the measured TEER values of co-cultures. The difference was multiplied with the filter area (1.12cm^2) and given as Ω*cm^2. TEER was measured for rBCECs in co-culture prior to transfection and again at the end of transfection.

The passive permeability was measured by the addition of 1µCi/ml 3H-D-Mannitol (Specific activity 15.9 Ci/mol) (Burkhart *et al.* 2015b; Thomsen *et al.* 2015) to the upper chamber of the filter insert at the end of the 24-hour transfection period. TEER was measured prior to the addition of Mannitol, and the cells were incubated for 2 hours at 37°C under mild agitation. During the incubation period donor samples (100µl) were taken from the upper chamber at 0 and 2 hours, while receiver samples (100µl) were taken from the lower chamber at 0, 15, 30, 60 and 120 min and replaced with equal amounts of fresh media. Samples were

added with Ultima Gold™ liquid scintillation cocktail and counted in a Hidex 300SL liquid scintillation counter (Kem-En-Rec Nordic, Taastrup, Denmark). The total amount of millimoles transported in each well was plotted against time and the flux at steady state calculated as the slope of the straight line divided by the area of the filter insert (1.12 cm^2). The apparent permeability (Papp) was then calculated by dividing the flux at steady state with the initial concentration in the donor upper compartment. The calculated Paap data were plotted against TEER values for each individual filter insert or collectively plotted regardless of TEER.

Transport of NPC2 across the BBB

NPC2 has been shown not to be able to cross the BBB *in vivo* (Nielsen *et al.* 2011), however, this might not be the case when studied *in vitro*. Therefore, the potential transport of NPC2 across the BBB was determined using the co-culture model. To study both the luminal to abluminal and abluminal to luminal transport (leakage) of NPC2, 5ng/ml human NPC2 standard (provided in the ELISA kit) were added to either the upper or the lower chamber at the point of high TEER. 24 hours later, media from the upper and lower chambers were collected and stored at -80°C for later analysis with ELISA.

Enzyme-Linked Immunosorbent Assay (ELISA)

The concentration of NPC2 in the media after transfection, the direction of secretion (upper or lower chamber), and the possible transport of NPC2 across the BBB was evaluated using an NPC2 ELISA pair kit based on a solid phase sandwich ELISA. All incubations were performed at room temperature, except when stated otherwise, under mild agitation. ELISA plates were incubated with 2µg/ml capture antibody in PBS (136.9 mM NaCl, 10.1 mM Na_2HPO_4, 2.7 mM KCl, 1.8 mM KH_2PO_4, pH 7.4) overnight at 4°C. The capture antibody was aspirated, and the plate washed three times in a wash buffer consisting of 0.05% Tween20 in TBS (20 mM Tris, 150 mM NaCl, pH 7.4) before being incubated with blocking buffer (2% BSA in wash buffer) for at least one hour. Prior to the addition of media samples, the blocking buffer was aspirated, and the plate washed three times. A seven-point standard curve using two-fold serial dilutions ranging from 10ng/ml to 0.156ng/ml was prepared as well. Standards were diluted in sample dilution buffer (0.1% BSA in wash buffer, pH 7.2 - 7.4). The plate was then incubated with media samples or standard for two hours. Samples and standards were aspirated, and the plate washed three times. 0.15µg/ml detection antibody diluted in antibody dilution buffer (0.5% BSA in wash buffer) was added and the plate incubated for another hour. The aspiration and washing steps were repeated before the addition of a substrate solution consisting of 10mg/ml TMB in DMSO and 3 % H_2O_2 diluted 1:100 and 1:1250, respectively, in substrate dilution buffer (0.05M Na_2HPO_4, 0.025M citric acid, pH 5.5). The reaction was stopped after 20 min incubation by the addition of 2 N H_2SO_4 and the optical density for each well determined using an EnSpire® Multimode Plate Reader (Perkin Elmer, Waltham MA, USA) set to

450nm. All samples and standards were measured in duplicates. Media served as blank to subtract the background. Data were analyzed with a computer-based curve-fitting software using a 4-parameter logistics curve-fitting algorithm, and the mean absorbance for each set of duplicates calculated (Elisaanalysis.com).

NPC2 protein replacement assay

NPC2 deficient fibroblasts are unable to transport cholesterol from the late-endosomal lysosomal system, due to the mutated NPC2 protein, which results in a major buildup of cholesterol inside the lysosomes in these cells. NPC2 deficient fibroblasts were therefore incubated with media from transfected cells (rBCECs in mono and co-culture or HeLa cells) for 48 hours to evaluate whether the transfection resulted in secretion of recombinant NPC2 to the media and if this secretion was able to correct the cholesterol buildup seen in these cells. Media from non-transfected cells were used as a control for endogenous secretion of NPC2, while 10µg/mL NPC2 purified from bovine milk (as described previously (Nielsen *et al.* 2011)) were used as a positive control. Wild-type fibroblasts served as a control for normal cholesterol amount inside cells and untreated NPC2 deficient fibroblast served as a control for non-treatment. Treated fibroblasts were subsequently used for immunocytochemistry.

Flow cytometry

Flow cytometry was used to assess the number of transfected rBCECs and HeLa cells in percentage and thereby the efficiency of the transfection assay. After the transfection period, the cells were washed twice in 0.1M PBS, pH 7.4 and detached from the culture support by trypsin and washed twice in PBS by spinning the sample at 300xG for 5 min. Cells from three wells in a 24 well plate or three hanging culture insert were pooled together to ensure enough cells for the analysis. The transfection efficiency was analyzed using CytoFLEX S (Beckman Coulter Copenhagen, DK)), which prior to the flow cytometric analysis was calibrated using CytoFLEX Daily QC Fluorospheres. Single-cell events were gated using forward and side scatters to eliminate cell debris and doublets. Approximately 50,000 cells were analyzed in each sample. Non-transfected cells were used as a control for autofluorescence. NPC2-OFPSpark positive cells were gated based on autofluorescence from the non-transfected cells to ensure less than 0.5 % false-positive events occurred. The results were analyzed using the CytExpert software (Beckman Coulter, Copenhagen, DK).

Immunocytochemistry and filipin III staining.

Immunocytochemistry was performed on rBCECs (mono and co-cultures), HeLa cells, and NPC2 deficient fibroblasts. All cells used for immunocytochemistry were either seeded on hanging filter inserts (rBCECs co-culture) or coverslips (rBCECs monoculture, HeLa Cells, and NPC2 deficient fibroblasts). The cells were washed twice in 0.1M PBS, fixed for 10 minutes in 4 % paraformaldehyde at room temperature and

washed twice in 0.1M PBS. The cells were blocked for unspecific binding in blocking buffer (3% BSA, 0.3% Triton-X-100 in 0.1M PBS) for 30 min. All incubations were performed at room temperature under mild agitation. rBCECs were incubated with primary antibodies against ZO1, ZO2, CLD5, OCLN, and NPC2, while HeLa cells were incubated with an anti-NPC2 antibody. Fibroblasts were incubated with primary antibodies against vimentin, MPR300, and NPC2. All antibodies were diluted (1:500 for vimentin and 1:250 for remaining antibodies) in blocking buffer for 1 hour. The cells were washed twice in washing buffer (blocking buffer diluted 1:50 in PBS, 0.1M pH 7) to remove unbound primary antibodies. Secondary Alexa flour 488 donkey anti-rabbit IgG, Alexa flour 594 goat anti-rabbit, and Alexa flour 488 goat anti-mouse IgG antibodies were diluted of 1:250 in blocking buffer and added to the cells for 1 hour. Secondary antibodies were aspirated, and the cells were washed twice in PBS. The nuclei were counterstained with DAPI (1:500 in PBS) in rBCECs and HeLa cells, while GelRed™ (1:10,000 in PBS) was used to counterstain the nuclei of fibroblasts. The fibroblasts were additionally incubated for one hour with 10 µg/mL filipin III diluted in PBS, added from a stock solution of 0.5mg/ml filipin III diluted in DMSO, followed by three washing steps in 0.1M PBS, pH 7. Filipin III binds specifically to free cholesterol and can, therefore, be used to assess cholesterol depositions in the cells. All cells were mounted on object slides using Dako Fluorescent mounting media. Antibody and filipin III staining, as well as OFP-Spark expression in genetically modified cells, was subsequently examined on an AxioObserver Z1 fluorescence microscope equipped with ApoTome and Axiocam MR camera under a Plan-Apochromat 40x/1.3 Oil DIC objective (rBCECs and HeLa cells) or a Plan-Apochromat 20x/0.8 DIC objective (fibroblasts). Acquired Images were corrected for brightness and contrast using the ImageJ software. The nuclei stain with GelRed™ was changed to blue to contrast the fluorescence of filipin III and fluorophores emitting at 488 nm.

Quantification of filipin III

Filipin III intensities were quantified to evaluate changes in the cholesterol load of NPC2 deficient fibroblasts and compared to WT fibroblasts. All fibroblasts used for quantification were stained with filipin III, GeldRed™ and antibodies against vimentin. For each situation in the NPC2 replacement assay, 8-11 different images were acquired for quantification. For image acquisition, only the vimentin staining was used to localize the cells to ensure blinded selection of areas. Filipin III exposure time was set based on untreated NPC2 deficient fibroblasts stained on the same day and kept constant for all situations. As it was not possible to stain all fibroblasts within a single run, untreated NPC2 deficient fibroblasts were included as an internal control in all filipin stainings. Filipin III intensities were measured using the ImageJ software as the sum of gray values in pixels above a defined pixel intensity threshold. The threshold was defined based on the pixel intensity histogram right after the first major peak, to exclude low filipin III intensities, caused by cholesterol in the cell membranes. Average filipin III intensities per cell were calculated for each

image to account for varying cell densities, based on automatic counting of nuclei using the particle analysis tool in ImageJ. Measured intensities for the different situations were subsequently normalized to the filipin III intensities of untreated NPC2 deficient fibroblasts stained on the same day, by calculating the filipin III intensity for different situations as percentage of the intensity of untreated NPC2 deficient fibroblasts. This was done in order to enable a comparison between intensities quantified from filipin III stainings carried out at different time points.

Statistics

Results are shown as mean with standard error of the mean (SEM). n values generally refer to number of filter inserts (co-culture model) or wells, as are further specified in the figure legends, except for data referring to Filipin III intensities, where n values refer to the number of images analyzed. All experiments were performed at least twice using cells from two different isolations of primary cells. No blinding was used, except for capturing images of fibroblasts used for quantification of filipin III, as described in the previous section. All statistical analysis was done using GraphPad Prism (version 6.0c) with a 0.05 significance level. No test for outliers was performed and no data points were excluded. All datasets containing a sample size above nine were analyzed for normality using a D'Agostino & Pearson omnibus normality test. Datasets that were normally distributed and had equal variances between the groups (analyzed using a F-test for datasets containing two groups and a Brown-Forsythe test for datasets containing more than two groups) were analyzed using a parametric unpaired t-test (Fig. 4d and 6e (RBEC mono)) or a parametric one-way ANOVA with Tukey's multiple comparisons post hoc test (Fig. 5d). Datasets that were not normally distributed (or not analyzed for normality) and found to have significantly different variances were all analyzed using a non-parametric Mann-Whitney test (Fig. 3b, 4b, 6b, 6c and 6e (HeLa)) or a non-parametric Kruskal-Wallis test with Dunn's multiple comparisons post hoc test (Fig. 1c). Datasets depicted in Fig. 5b were analyzed using a Brown-Forsythe test and found to have significantly different variances. However, for Fig. 5b significant differences in NPC2 secretions were only analyzed between the two groups' respective chambers (upper vs upper, and lower vs lower) using a non-parametric Mann-Whitney test. No statistical analysis was performed for data shown in Fig. 5a.

RESULTS

We have previously shown that non-dividing rBCECs cultured under *in vivo* like BBB conditions can become genetically modified to secrete recombinant proteins in the direction of both the blood and the brain using non-viral gene therapy (Burkhart *et al.* 2017; Burkhart *et al.* 2015b). We now wished to evaluate this strategy's potential in the treatment of the LSD Niemann-Picks disease type C2 caused by the small defective soluble enzyme, NPC2, normally involved in the transport of cholesterol within the late endosomal/lysosomal network (Vanier and Millat 2004). NPC2 deficient skin fibroblasts and WT fibroblasts were utilized to model the disease *in vitro*.

NPC2 deficient fibroblasts obtained from the skin of a patient suffering from Niemann Picks type C2 disease, carrying two different mutations and skin fibroblasts from a healthy person (WT) were characterized based on their expression of vimentin and the amount of cholesterol load inside the lysosomes (Fig. 1). Both NPC2 deficient fibroblasts and WT fibroblasts expressed the fibroblast marker, vimentin. When staining for cholesterol using filipin III, which binds specifically to cholesterol, a huge cholesterol build-up was seen around the nucleus of the NPC2 deficient fibroblasts, corresponding to the site of the lysosomes. This build-up was not observed in the WT fibroblasts, which have a functional NPC2 enzyme and, therefore, have a normal transport of cholesterol out of the late endosomal/lysosomal network (Fig. 1a). Both NPC2 deficient fibroblasts and WT fibroblasts expressed the MPR300 receptor involved in the transport of extracellular NPC2 into the endosomes (Storch and Xu 2009) (Fig. 1b). Accordingly, a previous study has shown that NPC2 isolated from bovine milk is able to correct the cholesterol load inside the NPC2 deficient fibroblasts (Nielsen *et al.* 2011). We, therefore, added 10µg/ml bNPC2 to the media of the NPC2 mutated fibroblasts, which resulted in a correction of cholesterol transport from the lysosomes to the same extent as that seen in the WT fibroblasts (Fig. 1a). When quantifying the cholesterol load inside the fibroblasts based on the fluorescent intensity of the filipin III stainings per cell, a significant difference was observed between the WT fibroblasts and the NPC2 deficient fibroblasts. The addition of 10µg/ml bNPC2 likewise resulted in a significant decrease in the cholesterol load compared to the NPC2 deficient fibroblasts. No significant difference was observed between WT fibroblasts and NPC2 deficient fibroblasts treated with 10µg/ml bNPC2 (Fig. 1c).

rBCECs were genetically modified to express human NPC2 coupled to an orange fluorescent tag (OFP). Before transfecting the rBCECs, we wanted to investigate the functionality of recombinant NPC2-OFP, due to the fact that the OFP tag is nearly twice the size of NPC2, and might, therefore, influence the synthesis of NPC2, the NPC2 receptor-mediated transport to the late endosomes, the binding of cholesterol to NPC2, or even the interplay between NPC1 and NPC2 inside the late endosomes (Fig. 7). We, therefore, transfected the NPC2 deficient fibroblasts to ensure an environment where no endogenous NPC2 was

present, and evaluated the cholesterol load in the transfected and neighboring cells 48 hours later, using filipin III stainings (Fig. 2). The fibroblasts were identified using vimentin staining, and positively transfected cells were recognized based on NPC2 immunocytochemistry. The non-transfected NPC2 deficient fibroblasts revealed high lysosomal cholesterol build-up and no expression of NPC2. Opposed to this, fibroblasts expressing NPC2-OFP exposed a clear reduction in cholesterol, suggesting that NPC2-OFP is functional (Fig. 2). Moreover, transfected NPC2 deficient fibroblasts seemed to have a slightly different morphology than the non-transfected NPC2 deficient fibroblasts. They were generally smaller and their spreading morphology in some cases seemed slightly retracted, which could indicate a negative response to the transfection or the recombinant protein in these cells, or simply that they are beginning to look more similar to the Wt cells. Due to low transfection efficiency, it was not possible to conclude that genetically modifying NPC2 deficient fibroblasts would secrete recombinant NPC2-OFP sufficiently to correct the cholesterol load in neighboring non-transfected cells (Fig. 2).

rBCECs in co-culture with astrocytes were then genetically modified to express the recombinant NPC2-OFP, and the transfection efficiency was evaluated based on a flow cytometric analysis (Fig. 3). Positively transfected rBCECs expressing NPC2-OFP could be recognized in a fluorescent microscope due to the OFP tag. NPC2-OFP expressing cells were only observed in the transfected cells. Double labeling using an NPC2 specific antibody revealed a clear co-localization between the OFP tag and recombinant NPC2 (Fig. 3a). The percentage of transfected rBCECs was counted to be 7.154 ± 0.24 % (Fig. 3b), corresponding well with that previously shown using a similar setup (Burkhart *et al.* 2017). To ensure the transfection did not affect the rBCECs ability to form and express tight junction proteins, we compared the protein expression of four important tight junction proteins, ZO1, ZO2, OCLN, and CLD5 between the two groups (Fig. 3c). Again, no NPC2-OFP expressing cells were observed in the non-transfected cells, but these cells showed robust expression of all four markers at the cell-cell junctions between neighboring cells. When the rBCECs were transfected the same robust expression was observed, both in the positively transfected cells and neighboring non-transfected cells, indicating that transfection did not affect the cells' ability to maintain their expression of the tight junction proteins ZO1, ZO2, OCLN, and CLD5 (Fig. 3c).

To further ensure that transfection did not affect the barrier integrity of the co-cultured rBCECs, we monitored TEER during transfection and calculated the Papp of the small molecule mannitol at the end of transfection (Fig. 4). rBCECs were co-cultured with astrocytes and exposed to several tight junctions inducing factors for 24 hours causing a dramatic increase in the TEER to values above 300 $\Omega*cm^2$ (333±12.7 $\Omega*cm^2$ for non-transfected rBCECs and 319.8±10.5 $\Omega*cm^2$ for transfected rBCECs). At this point in high TEER, transfection was initiated for 24 hours, and measures of TEER repeated. A slight decrease was observed in the transfected cells (298.3±7.5 $\Omega*cm^2$) and a slight increase observed in the non-transfected cells (337.7±8.4 $\Omega*cm^2$) (Fig. 4a). To evaluate if the difference were statistically significant, we

calculated the percentage decrease in both settings and found an 8.9% increase in TEER in the non-transfected cells and a 3.3% decrease in TEER in the transfected cells. Even though the transfected cells decreased, no significant difference was observed between the two groups, indicating that the decrease in TEER is not due to transfection (Fig. 4b). Likewise, the effect of transfection on the passive permeability of mannitol was investigated at the end of transfection. TEER was measured prior to the addition of mannitol. Both the transfected and non-transfected rBCECs showed high TEER values at the end of transfection (between 270 and 443 $\Omega*cm^2$) and the Papp for mannitol was in the range of $1.0*10^{-6}$ to $4.0*10^{-6}$ cm/s, suggesting a very low permeability (Gaillard and de Boer 2000; Burkhart *et al.* 2015b) (Fig. 4c). When looking at the individual filter inserts, no clear correlation indicates that higher TEER equals lower permeability, suggesting that within this TEER range, the permeability is generally low. Likewise, transfection did not seem to affect the permeability. When collectively comparing the permeability of mannitol between transfected ($2.55*10^{-6}\pm2.1*10^{-7}$ cm/s) and non-transfected cells ($2.32*10^{-6}\pm3.4*10^{-7}$ cm/s) no significant difference was observed (Fig. 4d).

Next, we wanted to evaluate if genetically modifying rBCECs resulted in secretion of recombinant NPC2 to the cell media and in which direction (upper chamber (blood) or lower chamber (brain)) the recombinant protein would be secreted (Fig. 5). In the literature NPC2 is not found to be able to cross the BBB *in vivo* (Nielsen *et al.* 2011), however, to ensure NPC2 is not transported across the BBB, or leaks between the two chambers in the *in vitro* BBB model, we analyzed the luminal to abluminal transport and vice versa of NPC2 (Fig. 5a). 5ng/ml (corresponding to 100%) was added to either the upper or the lower chamber and the concentration of NPC2 in all chambers was determined using an ELISA specific for NPC2. Only approximately 30% of the added concentration of NPC2 was recovered after 24 hours of incubation in the respective donor chambers (NPC2 added to the upper chamber: 31.4±0.8 %; NPC2 added to the lower chamber: 26.7±0.4 %) (Fig. 5a), suggesting a high uptake of NPC2 by the rBCECs and astrocytes. Despite the high uptake by the cells, no transport from luminal to abluminal or the reverse direction was observed, confirming the vivo data. Therefore, since NPC2 can not cross the *in vitro* BBB model, the amount of NPC2 secreted from the transfected rBCECs will be indicative of secretion and not due to leakage or transport between the two chambers. The secretion of NPC2 from the transfected rBCECs in co-culture with astrocytes could, therefore, be determined. Non-transfected rBCECs did not secrete NPC2 in either direction, however, 0.40±0.09ng/mL NPC2 was secreted in the direction of the upper chamber and 0.09±0.02ng/mL was measured in the lower chamber from transfected cells (Fig. 5b). The sampled media from both the upper and lower chamber was additionally added to the NPC2 deficient fibroblasts for 48 hours, after which their cholesterol content was evaluated using filipin III staining's (Fig. 5c). No visual difference was observed in the cholesterol load between untreated NPC2 deficient fibroblasts (Fig. 1a), NPC2 deficient fibroblasts treated with media from non-transfected cells, and NPC2 deficient fibroblasts

treated with media from transfected cells. Likewise, no difference was observed between NPC2 deficient fibroblasts treated with media from the upper or lower chambers. A high degree of cholesterol load was still observed inside the cells in all settings (Fig. 5b). Since it was difficult to evaluate the cholesterol load in the cells when the cholesterol is not completely removed, we further analyzed the cholesterol load in each condition based on the fluorescent intensity of the filipin III staining per cell, normalized to the intensity in untreated NPC2 deficient fibroblasts (Fig. 5d). Treating the NPC2 deficient fibroblasts with media from non-transfected cells (both upper and lower) did not result in any significant reduction in cholesterol load, which was also the case when treating the NPC2 deficient fibroblasts with media from transfected cells (both upper and lower chamber) (Fig. 5d). Hence, in spite transfected rBCECs indeed secreted NPC2 in both directions, its concentration in the current assay was not sufficiently high to signify an effect on the cholesterol load inside the NPC2 deficient fibroblasts.

With 7% of co-cultured rBCECs secreting NPC2 into the media, we hypothesized that increasing the transfection efficiency would accordingly increase the concentration of recombinant NPC2 being secreted into the media to a concentration where the cholesterol load inside the NPC2 deficient fibroblasts would be corrected. rBCECs in co-culture secreted recombinant NPC2 in the range of pg/ml, while a complete correction of cholesterol using bNPC2 was obtained in the range of µg/ml. We have previously shown that rBCECs not cultured under *in vivo* BBB like settings, i.e. a simple monoculture on the bottom of a well without the influence of BBB inducing factors and astrocytes, shows higher transfection efficiency using the transfection agent Lipofectamine 3000™ than rBCECs in co-culture, in spite of their post-mitotic status (Burkhart *et al.* 2017). Moreover, HeLa cells can very effectively be transfected using this transfection agent (Burkhart *et al.* 2017). We, therefore, transfected both rBCECs in monoculture (rBCECs (mono)) and HeLa cells, analyzed the transfection efficiency and sampled the media for ELISA and treatment of NPC2 deficient fibroblasts (Fig. 6). Only NPC2-OFP expressing cells were observed in the transfected rBCECs (mono) and transfected HeLa cells. rBCECs (mono) was, additionally, recognized by their expression of ZO1, which were found in both transfected and non-transfected rBCECs (Fig. 6a). However, the expression of ZO1 was not as organized as that observed in the co-cultured rBCECs (Fig. 4c). The transfection efficiency was 21.1±3.8 % for rBCECs (mono) and 74.6±2.4 % for HeLa cells (Fig. 6b), which resulted in secretion of recombinant NPC2 from the transfected cells into the media in a concentration of 3.3±0.7% ng/ml and 16±1.7ng/ml respectively (Fig. 6c). Non-transfected cells did not secrete NPC2 into the media. The addition of media from the transfected and non-transfected rBCECs (mono) to the NPC2 deficient fibroblasts for 48 hours resulted in partly correction of the cholesterol load for the fibroblasts treated with media from the transfected rBCECs (mono), while no correction was seen in the cells treated with media from the non-transfected rBCECs (mono) (Fig. 6d). When quantifying the cholesterol load based on the fluorescent intensity of the filipin III staining per cell a significant decrease is observed when media from

transfected rBCECs (mono) were added compared to fibroblasts treated with media from non-transfected rBCECs (Fig. 6e). When adding media from transfected HeLa cells to the NPC2 deficient fibroblast a complete correction in the cholesterol load was observed, which is not the case when adding media from the non-transfected HeLa cells (Fig. 6d). This complete correction of cholesterol load was confirmed when quantifying the cholesterol load based on the fluorescent intensity of the filipin III staining per cell. The addition of media from transfected HeLa cells resulted in complete correction of the cholesterol load to the same extent as that seen in the WT fibroblasts (Fig. 1c) compared to NPC2 deficient fibroblasts treated with media som non-transfected HeLa cells (Fig. 6e). Therefore, increasing the transfection efficiency was crucial for ensuring sufficient amount of NPC2 in order to correct the cholesterol load in NPC2 deficient fibroblasts.

DISCUSSION

Secretion of recombinant NPC2 protein from transfected rBCECs

In this study, we demonstrate that primary rBCECs can be genetically modified using the non-viral vector Lipofectamine 3000™ in an *in vitro* BBB model with a transfection efficiency of 7 % without compromising the barrier integrity with regards to the expression of the tight junction proteins ZO1, ZO2, OCLN, and CLD5, TEER, and passive permeability to mannitol. It might be questionable whether 7 % of transfected cells would be enough to exert an effect on the tightness of the rBCECs cell layer. However, the expression of the examined tight junction proteins does not seem altered in transfected cells compared to non-transfected cells and neither does the overall passive permeability to a small molecule like mannitol, which would presumably pass through the cell layer in case of leakage around transfected cells. Even though transfection did not affect the barrier integrity, it can not be excluded that other aspects of the cells' BBB characteristics (eg. expression or trafficking of receptors) could be affected. The secretion of recombinant NPC2 from transfected rBCECs in co-cultures with astrocytes was too low to induce a biological effect on NPC2 deficient fibroblasts. However, an increased transfection efficiency could be achieved on monocultures, which in turn increased the recombinant NPC2 secretion to a level significant to demonstrate biological effects. This observation confirms the findings of a previous study by Burkhart et al., where we were able to induce secretion of recombinant erythropoietin from primary rBCECs in a similar *in vitro* BBB model, with an efficiency of 8 %, without compromising the barrier integrity, following transfection with Lipofectamine 3000™ (Burkhart *et al.* 2017). The secretion from transfected rBCECs resulted in NPC2 concentrations of 0.4 ng/mL±0.09 in the upper chamber and 0.09ng/mL±0.02 in the lower chamber, while our previous study resulted in erythropoietin secretions leading to 1.47 ng/mL and 0.13 ng/mL in the upper and lower chambers, respectively (Burkhart *et al.* 2017). The secretion of NPC2 from transfected primary rBCECs thus appears slightly reduced compared to the secretion of erythropoietin. However, converting these concentrations to molar concentrations reveals higher secretion to the lower chamber of 5.29 nM NPC2 (MW 17kD) compared to 3.83 nM erythropoietin (MW 34kD), while the molar concentrations of erythropoietin (43.2nM) in the upper chamber still remains higher than of NPC2 (23.5nM).

Mannose-6-phosphate (M6P) is a distinctive post-translational modification critical for the trafficking of NPC2. Under normal conditions, the majority of newly synthesized NPC2 is transported from the Golgi to the lysosomes, while only a smaller amount is secreted from the cell (Sands and Davidson 2006) (Fig. 7). A similar distribution of recombinant NPC2 produced following transfection could explain why a transfection efficiency similar to that previously observed for erythropoietin using a similar setup would result in less recombinant protein secreted to the cell media in the case of NPC2. Moreover, as the endothelial cells

present the M6P receptor MPR300 on the plasma membrane, for which NPC2 is a natural ligand, there might be a re-uptake of secreted recombinant NPC2, which would decrease the extracellular even more (Siupka *et al.* 2017; Nielsen *et al.* 2001). The results of the NPC2 transport study strongly supports this, as only around 30% of added NPC2 protein could be retrieved from the media after 24 hours of incubation. Secretions of recombinant NPC2 from transfected cells may, therefore, be even higher than what we were able to measure in the media 24 hours post-transfection.

Due to the low secretion of recombinant NPC2, we were unable to detect a biologic effect of the recombinant NPC2 secreted from transfection of 7% of the primary rBCECs in co-cultures contrary to our previous findings with secreted recombinant erythropoietin following transfection of 8% of the primary rBCECs (Burkhart *et al.* 2017). The results from the transfection of rBCECs in co-cultures thus demonstrate that higher transfection efficiency is needed to induce a biological effect of secreted recombinant NPC2, which was further supported by the findings from transfection of primary rBCECs in monocultures and HeLa cells. Corresponding to previous findings, transfection of primary rBCECs in monocultures and HeLa cells leads to markedly increased transfection efficiencies (Burkhart *et al.* 2017), which results in increased secretion of recombinant NPC2 inducing a partly and complete reversal of the cholesterol accumulations in NPC2 deficient fibroblasts following incubation with conditioned medium from transfected rBCECs in monocultures and HeLa cells, respectively (Fig. 6d and 6e). However, this leads to the question about, which levels of NPC2 are needed to correct the pathological cholesterol load in deficient cells lacking functional NPC2 expression. Nielsen et al. previously demonstrated a complete reversal of cholesterol accumulations in deficient NPC2 fibroblasts following incubation with 10 µg/mL bNPC2 purified from milk, which was also confirmed in the current study (Nielsen *et al.* 2011). Moreover, in the study by Nielsen et al. they report that a similar effect was observed when reducing the concentration of bNPC2 10-fold (Nielsen *et al.* 2011). However, our results demonstrate a complete reversal of cholesterol accumulations in deficient NPC2 fibroblasts following treatment with medium from transfected HeLa cells containing only 16 ng/mL of recombinant NPC2. A possible explanation for this could be the species differences between human and bNPC2. However, NPC2 has previously been shown to be a highly conserved protein between species with an almost complete similarity between all functionally essential regions (Friedland *et al.* 2003; Nielsen *et al.* 2011). In addition to that, we initially discovered a surprisingly high concentration of NPC2 in the bovine PDS normally used in the culture medium for primary BCECs (Burkhart *et al.* 2015b; Thomsen *et al.* 2017; Thomsen *et al.* 2015). Initial control experiments revealed a markedly reduced cholesterol load in NPC2 deficient fibroblasts following addition of unconditioned rBCEC medium supplemented with 10% PDS, corresponding to NPC2 concentrations of approximately 1 ng/mL when measured with ELISA (data not shown), which led to a substitution of PDS with FCS in the rBCEC culture medium used for transfection. Nevertheless, these findings indicate that a

beneficial biological effect can possibly be induced by even lower extracellular concentrations of NPC2 than those observed from rBCEC monocultures and HeLa cells in the present study.

It has previously been argued that a therapeutic effect can be induced in lysosomal storage diseases by the addition of less than 10 % of the normal level of lysosomal protein (Sands and Davidson 2006). Moullier et al. demonstrated that lysosomal storage could be reversed in the liver of a mouse model of Mucopolysaccharidosis VII by induction of only 0.8–2.4 % of normal enzyme activity (Moullier *et al.* 1993). However, it is uncertain whether this would be the case in all lysosomal storage diseases. Moreover, in the case of NPC2, which is a very rare disease (Vanier 2010), only very few studies have examined what the NPC2 protein concentrations in healthy individuals are, and most of these only report whether the protein is present or not. One study examined the NPC2 protein expression in multiple cancers, compared to healthy adults (Liao *et al.* 2013). Even though their study mainly focuses on relative NPC2 protein concentrations, they demonstrated a NPC2 human serum concentration of 3.29 ng/mL in healthy controls (Liao *et al.* 2013). This concentration correlates well with the recombinant protein secretions observed in the present study following transfection of rBCECs in monocultures with a 20 % efficiency. However, it is difficult to make any conclusions regarding the concentrations needed to exert a biological effect in deficient cells based on serum concentrations from healthy controls. Thus, it remains uncertain exactly which NPC2 concentration and hence what gene modification efficiencies are needed to induce a beneficial biological effect of the NPC2 gene therapy. Nevertheless, the idea of using genetically modified cells to rescue NPC2 deficient cells remains promising, as we were able to reverse the cholesterol accumulations in NPC2 deficient fibroblasts partly by addition of recombinant NPC2 secreted from genetically modified BCECs and completely by addition of recombinant NPC2 secreted from genetically modified HeLa cells.

To further evaluate the potential of using BCECs to secrete NPC2 to the blood and CNS it would be interesting to investigate the effect of secretions from the genetically modified BCECs on NPC2 deficient neurovascular cells like neurons, astrocytes, BCECs, microglia rather than fibroblasts, as it is uncertain whether these cells might be more or less receptive to the addition of recombinant extracellular NPC2. A number of studies have previously described the potential of developing induced pluripotent stem cells from fibroblasts with the aim of developing improved disease models, especially in the case of monogenic diseases (Takahashi and Yamanaka 2006; Vatine *et al.* 2017; Appelt-Menzel *et al.* 2017; Mattis *et al.* 2014; Yu *et al.* 2007). Future studies focusing on developing induced pluripotent stem cells from the NPC2 deficient fibroblasts used in the present study, would thus provide an opportunity to study both the potential effects of recombinant NPC2 secreted from genetically modified cells on relevant CNS cells as well as the effects of the gene modification itself on an NPC2 deficient *in vitro* BBB model.

Gene therapy as a drug delivery strategy for transport through the BBB

In this study, we have investigated the potential of genetically modifying BCECs to secrete NPC2, as a strategy for CNS delivery using a non-viral vector, as illustrated in Fig. 7. However, the non-viral gene modification of BCECs in an *in vitro* BBB model with defined BBB properties resulted in insufficient secretion of NPC2. Therefore, further evaluation of this strategy requires increased gene modification efficiency. Non-viral gene therapy requires a carrier that ensures stability within the bloodstream to induce efficient delivery of the genetic material. In addition to that, the gene therapy vector should be able to induce cellular uptake of the genetic material in the target cell, followed by the release of the genetic material within the cell (Rezaee *et al.* 2016; Jayant *et al.* 2016), a process often referred to as endosomal escape. Finally, the genetic material needs to be transported to the cell nucleus to ensure transcription of the genetic material (Jayant *et al.* 2016; Rezaee *et al.* 2016), which is believed to take place either through nuclear membrane pores or during cell division when the nuclear envelope is temporarily disassembled (Lechardeur *et al.* 2005; Lechardeur and Lukacs 2002). On the contrary, some viral vectors are naturally capable of efficiently by-passing cellular membranes in order to transport their genetic material to the cell nucleus, making such vectors less dependent on cell division (Choudhury *et al.* 2017). Furthermore, some viral vectors are capable of inducing long-term gene expression, while non-viral transfections only lead to transient transgene expression (Gan *et al.* 2013; Choudhury *et al.* 2017).

Though non-viral gene therapy vectors possess attractive safety properties (Choong *et al.* 2016; Simonato *et al.* 2013), the results of this study strongly underline the need for efficient gene modification in order to ensure sufficient production of recombinant protein to induce therapeutic effects. In addition to that, an increased transfection efficiency would be essential when moving to *in vivo* studies to ensure BCEC secretion throughout the entire CNS as well as sufficient secretion to the bloodstream to ensure distribution to all other organs in the case of Niemann Picks type C2 disease. An increasing number of studies have demonstrated successful treatment of animal models of other neurologic diseases with systemic involvements following intracisternal administration of gene therapies (Gray *et al.* 2013; Roca *et al.* 2017; Bey *et al.* 2017; Haurigot *et al.* 2013; Markmann *et al.* 2018). Notably, all of the gene therapy approaches used in these studies are based on the non-pathogenic AAVs, which express very low immunogenicity (Bessis *et al.* 2004). Today, these vectors represent the most commonly used vectors for CNS clinical trials (Choudhury *et al.* 2017; Gan *et al.* 2013). In addition to very low immunogenicity, results from several studies have revealed promising long-term episomal transgene expressions, particularly in slowly or non-dividing cells, following AAV mediated gene transfer (Körbelin *et al.* 2016; Hadaczek *et al.* 2010; Leone *et al.* 2012). Leone et al. demonstrated transgene expression for more than 10 years in the human brain following administration of an AAV serotype 2 vector (Leone *et al.* 2012).

When moving to *in vivo* studies it would additionally be very important to consider the biodistribution of the vector following systemic injections as well as the duration of transgene expression. Specific targeting

of the BCECs would be crucial to ensure especially protein secretion to the CNS. Synthesis of a non-viral carrier, which specifically targets the BCECs, has been proven to be very difficult (Johnsen *et al.* 2017; Johnsen and Moos 2016), whereas some viral vectors have the advantage of containing different natural tissue tropisms, which can be exploited in the development of a targeted gene therapy vector (Choudhury *et al.* 2017; Gan *et al.* 2013). This is especially true for the AAV vectors, which includes a large number of different serotypes with different tissue tropism (Saraiva *et al.* 2016). However, accumulation in especially liver tissue with the potential induction of hepatocellular carcinomas has been observed following systemic injections of AAV vectors (Gray *et al.* 2010; Chen *et al.* 2009; Körbelin *et al.* 2016; Donsante *et al.* 2001). Hence, efforts have been made to modify the natural tropism of these vectors to increase the specificity even more, including *in vivo* screening of random virus display peptide libraries or the insertion of phage selected peptides or ligands (Chen *et al.* 2009; Münch *et al.* 2013; Michelfelder *et al.* 2009). In a recent study by Körbelin et al. the targeting specificity of an AAV2 vector, developed from *in vivo* screening of a random AAV2 peptide library, has been demonstrated to induce efficient and brain endothelial cell-specific transgene expression following intravenous administration in mice (Körbelin *et al.* 2016). They presented a 1,000-fold higher transgene expression in brain tissue following intravenous administration compared to liver tissue, with the recombinant protein expression being practically invisible in the liver with *in vivo* luminescence imaging, while the expression in the brain was clearly visible, indicating a very brain-specific vector. Moreover, they were able to demonstrate a 650-fold higher transgene expression in the brain compared to a wild type AAV2 vector, which remained at the same level during a study period of more than 660 days (Körbelin *et al.* 2016). Combining these results with the generally attractive safety features of AAV vectors, this BCEC specific AAV2 vector studied by Körbelin et al. hence could represent a favorable vector candidate for the future development of the NPC2 gene therapy strategy investigated in the current study.

Furthermore, it will be interesting to further evaluate the secretion direction from genetically modified BCECs, as this is considered particularly relevant for the strategy proposed in this study. Although *in vitro* studies of the direction of secretion might not represent the *in vivo* situation completely, it enables precise quantification of the secretion of the transgene to the blood and brain side of the BBB. Former studies have revealed some controversy concerning the main secretory direction (Burkhart *et al.* 2017; Jiang *et al.* 2003). In the study by Jiang et al., glial-derived neurotrophic factor secretion was detected following transfection of a mouse brain endothelial cell line (MBEC4). They used MBEC4s monocultures seeded on Transwell ® filters as an *in vitro* BBB model in which they observed secretion primarily to the brain side (Jiang *et al.* 2003). On the contrary, the previously mentioned study by Burkhart et al. showed secretion of recombinant erythropoietin mainly to the blood side following transfection of primary rBCECs co-cultured with primary astrocytes in an *in vitro* BBB model (Burkhart *et al.* 2017) consistent with our findings. The *in vitro* BBB

model used by Burkhart et al. most closely mimics the *in vivo* situation as it includes both primary endothelial cells and astrocytes (Burkhart *et al.* 2017). However, it is unsure whether this would still be the case when moving to *in vivo* studies.

Although additional studies are still needed to completely assess the possibility of using gene therapy on BCECs to induce protein secretion to the CNS, the possible applications of this strategy are not limited to the treatment of Niemann Picks type C2 disease. Even though Niemann Picks type C2 disease is a very rare disease, it belongs to a large group of lysosomal storage diseases with a total incidence of 1:6700 (Sands and Haskins 2008). 75% of these, involve CNS symptoms, emphasizing a crucial need for delivery of drugs to the CNS (Sands and Haskins 2008). Many of these diseases are caused by a deficiency of a soluble protein similar to the situation in Niemann Picks type C2 disease. Examples of these are Gaucher's disease, Mucopolysaccharidosis types I, II and VI, and Pompe disease, (Sands and Davidson 2006; Beck 2009). Thus the genetic modification of BCECs to induce production and secretion of proteins to the CNS could denote an effective treatment strategy in several lysosomal storage diseases with a slight modification to fit the different diseases (Sands and Davidson 2006). Moreover, the strategy could potentially be relevant in other major CNS diseases; however, in diseases solely affecting the CNS secretions to the blood side of the BBB could lead to potential side effects depend on the therapeutic protein, which would need to be carefully considered. Nevertheless, based on the findings of the present study, using gene therapy on BCECs as a strategy for delivery of therapeutic proteins to the brain still seems promising but would require a higher transfection efficiency, which could probably be achieved by using a viral vector specifically targeting the BBB for future *in vivo* studies.

In conclusion, we have demonstrated that primary BCECs can be transfected to induce secretion of recombinant NPC2 across the BBB. Gene modification of primary BCECs in co-culture with primary astrocytes did not seem to compromise the barrier integrity of the BCECs. Moreover, we were able to demonstrate a biological effect of recombinant NPC2 secreted from transfected BCECs on NPC2 deficient fibroblasts, resulting in a partial reversal of the cholesterol accumulation in these cells. The effect was increased even further to a complete reversal of cholesterol accumulations in NPC2 deficient cells by increasing the transfection efficiency in HeLa cells. Thus, using gene therapy on BCECs as a strategy to induce secretion of NPC2 across the BBB seems very promising, but obtaining high transfection efficiencies is crucial in order to achieve sufficient biological effects.

Involves human subjects:

If yes: Informed consent & ethics approval achieved:

=> if yes, please ensure that the info "Informed consent was achieved for all subjects, and the experiments were approved by the local ethics committee." is included in the Methods.

ARRIVE guidelines have been followed:

Yes

=> if it is a Review or Editorial, skip complete sentence => if No, include a statement in the "Conflict of interest disclosure" section: "ARRIVE guidelines were not followed for the following reason:

"

(edit phrasing to form a complete sentence as necessary).

=> if Yes, insert in the "Conflict of interest disclosure" section:

"All experiments were conducted in compliance with the ARRIVE guidelines." unless it is a Review or Editorial

Conflicts of interest: none

=> if 'none', insert "The authors have no conflict of interest to declare."

=> otherwise insert info unless it is already included

ACKNOWLEDGEMENTS

This work was funded by generous grants from the Research Initiative on Blood-Brain Barrier and Drug Delivery founded by the Lundbeck Foundation (Grant no: 2013-14113), Fonden for Lægevidenskabens Fremme, Lily Benthine Lunds fond af 1.6.1978, Torben og Alice Frimodts Fond, Læge Sophus Carl Emil Friis

og Hustru Olga Doris Friis Legat, Oda og Hans Svennings Fond, Hørslev Fonden, and Civilingeniør Frode V. Nyegaard og Hustrus Fond. We want to thank Hanne Krone Nielsen and Merete Fredsgaard, Aalborg University, Denmark and Margit Skriver Rasmussen, Aarhus University for excellent technical assistance. We would also like to thank Brita Holst for expert assistance in operating the Cytoflex flow cytometer system. Kasper Bendix Johnsen is thanked for graphical assistance with Figure 7. We have no conflict of interest to declare.

REFERENCES

Abbott N. J., Patabendige A. A. K., Dolman D. E. M., Yusof S. R., Begley D. J. (2009) Structure and function of the blood–brain barrier. *Neurobiol. Dis.* **37**, 13–25.

Abbott N. J., Rönnbäck L., Hansson E. (2006) Astrocyte–endothelial interactions at the blood–brain barrier. *Nat. Rev. Neurosci.* **7**, 41–53.

Alvarez J. I., Dodelet-Devillers A., Kebir H., Ifergan I., Fabre P. J., Terouz S., Sabbagh M., et al. (2011) The Hedgehog pathway promotes blood-brain barrier integrity and CNS immune quiescence. *Science (80-.).* **334**, 1727–31.

Appelt-Menzel A., Cubukova A., Günther K., Edenhofer F., Piontek J., Krause G., Stüber T., Walles H., Neuhaus W., Metzger M. (2017) Establishment of a Human Blood-Brain Barrier Co-culture Model Mimicking the Neurovascular Unit Using Induced Pluri- and Multipotent Stem Cells. *Stem Cell Reports* **8**, 894–906.

Armulik A., Genové G., Mäe M., Nisancioglu M. H., Wallgard E., Niaudet C., He L., et al. (2010) Pericytes regulate the blood–brain barrier. *Nature* **468**, 557–561.

Ashtari N., Jiao X., Rahimi-Balaei M., Amiri S., E. Mehr S., Yeganeh B., Marzban H. (2016) Lysosomal Acid Phosphatase Biosynthesis and Dysfunction: A Mini Review Focused on Lysosomal Enzyme Dysfunction in Brain. *Curr. Mol. Med.* **16**, 439–446.

Assmann J. C., Körbelin J., Schwaninger M. (2016) Genetic manipulation of brain endothelial cells in vivo. *Biochim. Biophys. Acta - Mol. Basis Dis.* **1862**, 381–394.

Beck M. (2009) Therapy for lysosomal storage disorders. *IUBMB Life* **62**, 33–40.

Bessis N., GarciaCozar F. J., Boissier M.-C. (2004) Immune responses to gene therapy vectors: influence on vector function and effector mechanisms. *Gene Ther.* **11**, S10–S17.

Bey K., Ciron C., Dubreil L., Deniaud J., Ledevin M., Cristini J., Blouin V., Aubourg P., Colle M.-A. (2017) Efficient CNS targeting in adult mice by intrathecal infusion of single-stranded AAV9-GFP for gene therapy of neurological disorders. *Gene Ther.* **24**, 325–332.

Burkhart A., Andresen T. L., Aigner A., Thomsen L. B., Moos T. (2017) Transfection of primary brain capillary endothelial cells for protein synthesis and secretion of recombinant erythropoietin: a strategy to enable protein delivery to the brain. *Cell. Mol. Life Sci.* **74**, 2467–2485.

Burkhart A., Skjørringe T., Johnsen K. B. K. B., Siupka P., Thomsen L. B., Nielsen M. S., Thomsen L. L., Moos T. (2015a) Expression of iron-related proteins at the neurovascular unit supports reduction and reoxidation of iron for transport through the blood-brain barrier. *Mol. Neurobiol.* **53**, 7237–7253.

Burkhart A., Thomsen L. B., Thomsen M. S., Lichota J., Fazakas C., Krizbai I., Moos T. (2015b) Transfection of brain capillary endothelial cells in primary culture with defined blood–brain barrier properties. *Fluids Barriers CNS* **12**, 1–14.

Calabria A. R., Weidenfeller C., Jones A. R., Vries H. E. De, Shusta E. V. (2006) Puromycin-purified rat brain microvascular endothelial cell cultures exhibit improved barrier properties in response to glucocorticoid induction . *J. Neurochem.* **97**, 922–933.

Chen Y. H., Chang M., Davidson B. L. (2009) Unique molecular signatures of disease brain endothelia provide - a novel site for CNS-directed enzyme therapy. *Nat. Med.* **15**, 1215–1218.

Choong C.-J., Baba K., Mochizuki H. (2016) Gene therapy for neurological disorders. *Expert Opin. Biol. Ther.* **16**, 143–159.

Choudhury S. R., Hudry E., Maguire C. A., Sena-Esteves M., Breakefield X. O., Grandi P. (2017) Viral vectors for therapy of neurologic diseases. *Neuropharmacology* **120**, 63–80.

Daneman R., Zhou L., Kebede A. A., Barres B. A. (2010) Pericytes are required for blood–brain barrier integrity during embryogenesis. *Nature* **468**, 562–566.

Déglon N., Hantraye P. (2005) Viral vectors as tools to model and treat neurodegenerative disorders. *J. Gene Med.* **7**, 530–539.

Donsante A., Vogler C., Muzyczka N., Crawford J., Barker J., Flotte T., Campbell-Thompson M., Daly T., Sands M. (2001) Observed incidence of tumorigenesis in long-term rodent studies of rAAV vectors. *Gene Ther.* **8**, 1343–1346.

Fratantoni J. C., Hall C. W., Neufeld E. F. (1968) Hurler and Hunter Syndromes: Mutual Correction of the Defect in Cultured Fibroblasts. *Sci. New Ser.* **162**, 570–572.

Friedland N., Liou H.-L., Lobel P., Stock A. M. (2003) Structure of a cholesterol-binding protein deficient in Niemann-Pick type C2 disease. *PNAS* **100**, 2512–7.

Gaillard P. J., Boer A. G. de (2000) Relationship between permeability status of the blood-brain barrier and in vitro permeability coefficient of a drug. *Eur. J. Pharm. Sci.* **12**, 95–102.

Gan Y., Zheng J., Stetler R. A., Cao G. (2013) Gene delivery with viral vectors for cerebrovascular diseases. *Front Biosci (Elite Ed)* **5**, 188–203.

Gray S. J., Nagabhushan Kalburgi S., McCown T. J., Jude Samulski R. (2013) Global CNS gene delivery and evasion of anti-AAV-neutralizing antibodies by intrathecal AAV administration in non-human primates. *Gene Ther.* **20**, 450–9.

Gray S. J., Woodard K. T., Samulski R. J. (2010) Viral vectors and delivery strategies for CNS gene therapy. *Ther. Deliv.* **1**, 517–34.

Hadaczek P., Eberling J. L., Pivirotto P., Bringas J., Forsayeth J., Bankiewicz K. S. (2010) Eight years of clinical improvement in MPTP-lesioned primates after gene therapy with AAV2-hAADC. *Mol. Ther.* **18**, 1458–61.

Haurigot V., Marcó S., Ribera A., Garcia M., Ruzo A., Villacampa P., Ayuso E., et al. (2013) Whole body correction of mucopolysaccharidosis IIIA by intracerebrospinal fluid gene therapy. *J. Clin. Invest.* **123**, 3254–3271.

Jayant R. D., Sosa D., Kaushik A., Atluri V., Vashist A., Tomitaka A., Nair M. (2016) Current status of non-viral gene therapy for CNS disorders. *Expert Opin. Drug Deliv.* **13**, 1433–45.

Jiang C., Koyabu N., Yonemitsu Y., Shimazoe T., Watanabe S., Naito M., Tsuruo T., Ohtani H., Sawada Y. (2003) In Vivo Delivery of Glial Cell-Derived Neurotrophic Factor Across the Blood–Brain Barrier by Gene Transfer into Brain Capillary Endothelial Cells. *Hum. Gene Ther.* **14**, 1181–1191.

Johnsen K. B., Burkhart A., Melander F., Kempen P. J., Vejlebo J. B., Siupka P., Nielsen M. S., Andresen T. L., Moos T. (2017) Targeting transferrin receptors at the blood-brain barrier improves the uptake of immunoliposomes and subsequent cargo transport into the brain parenchyma. *Sci. Rep.* **7**, 10396.

Johnsen K. B., Moos T. (2016) Revisiting nanoparticle technology for blood–brain barrier transport: Unfolding at the endothelial gate improves the fate of transferrin receptor-targeted liposomes. *J. Control. Release* **222**, 32–46.

Körbelin J., Dogbevia G., Michelfelder S., Ridder D. A., Hunger A., Wenzel J., Seismann H., et al. (2016) A brain microvasculature endothelial cell-specific viral vector with the potential to treat neurovascular and neurological diseases. *EMBO Mol. Med.* **8**, 609–25.

Lechardeur D., Lukacs G. L. (2002) Intracellular barriers to non-viral gene transfer. *Curr. Gene Ther.* **2**, 183–94.

Lechardeur D., Verkman A., Lukacs G. (2005) Intracellular routing of plasmid DNA during non-viral gene transfer. *Adv. Drug Deliv. Rev.* **57**, 755–767.

Leone P., Shera D., McPhee S. W. J., Francis J. S., Kolodny E. H., Bilaniuk L. T., Wang D.-J., et al. (2012) Long-term follow-up after gene therapy for canavan disease. *Sci. Transl. Med.* **4**, 165ra163.

Liao Y.-J., Lin M.-W., Yen C.-H., Lin Y.-T., Wang C.-K., Huang S.-F., Chen K.-H., et al. (2013) Characterization of Niemann-Pick Type C2 protein expression in multiple cancers using a novel NPC2 monoclonal antibody. *PLoS One* **8**, e77586.

Lim-Melia E. R., Kronn D. F. (2009) Current enzyme replacement therapy for the treatment of lysosomal storage diseases. *Pediatr. Ann.* **38**, 448–455.

Markmann S., J. Christie-Reid J., Rosenberg J. B., De B. P., Kaminsky S. M., Crystal R. G., Sondhi D. (2018) Attenuation of the Niemann-Pick type C2 disease phenotype by intracisternal administration of an AAVrh.10 vector expressing Npc2. *Exp. Neurol.* **306**, 22–33.

Mattis V. B., Tom C., Akimov S., Saeedian J., Østergaard M. E., Southwell A. L., Doty C. N., et al. (2014) HD iPSC-derived neural progenitors accumulate in culture and are susceptible to BDNF withdrawal due to glutamate toxicity. *Hum. Mol. Genet.* **24**, 3257–3271.

Michelfelder S., Kohlschütter J., Skorupa A., Pfennings S., Müller O., Kleinschmidt J. A., Trepel M. (2009) Successful expansion but not complete restriction of tropism of adeno-associated virus by in vivo biopanning of random virus display peptide libraries. *PLoS One* **4**, e5122.

Misje Mathiisen T., Lehre K. P., Christian Danbolt N., Petter Ottersen O. (2010) The Perivascular Astroglial Sheath Provides a Complete Covering of the Brain Microvessels: An Electron Microscopic 3D Reconstruction. *Glia* **58**, 1094–1103.

Moullier P., Bohl D., Heard J.-M., Danos O. (1993) Correction of lysosomal storage in the liver and spleen of MPS VII mice by implantation of genetically modified skin fibroblasts. *Nat. Genet.* **4**, 154–159.

Münch R. C., Janicki H., Völker I., Rasbach A., Hallek M., Büning H., Buchholz C. J. (2013) Displaying high-affinity ligands on adeno-associated viral vectors enables tumor cell-specific and safe gene transfer. *Mol. Ther.* **21**, 109–18.

Nielsen G. K., Dagnaes-Hansen F., Holm I. E., Meaney S., Symula D., Andersen N. T., Heegaard C. W. (2011) Protein replacement therapy partially corrects the cholesterol-storage phenotype in a mouse model of Niemann-Pick type C2 disease. *PLoS One* **6**, e27287.

Nielsen M. S., Madsen P., Christensen E. I., Nykjaer A., Gliemann J., Kasper D., Pohlmann R., Petersen C. M. (2001) The sortilin cytoplasmic tail conveys Golgi-endosome transport and binds the VHS domain of the GGA2 sorting protein. *EMBO J.* **20**, 2180–90.

Pardridge W. M. (2005) The blood-brain barrier: Bottleneck in brain drug development. *Am. Soc. Exp. Neurother.* **2**, 3–14.

Patterson C. M., Walkley U. S. (2017) Niemann-Pick disease, type C and Roscoe Brady. *Mol. Genet. Metab.* **120**, 34–37.

Perrière N., Demeuse P. H., Garcia E., Regina A., Debray M., Andreux J. P., Couvreur P., et al. (2005) Puromycin-based purification of rat brain capillary endothelial cell cultures. Effect on the expression of blood-brain barrier-specific properties . *J. Neurochem.* **93**, 279–289.

Rezaee M., Oskuee R. K., Nassirli H., Malaekeh-Nikouei B. (2016) Progress in the development of lipopolyplexes as efficient non-viral gene delivery systems. *J. Control. Release* **236**, 1–14.

Roca C., Motas S., Marcó S., Ribera A., Sánchez V., Sánchez X., Bertolin J., et al. (2017) Disease correction by AAV-mediated gene therapy in a new mouse model of mucopolysaccharidosis type IIID. *Hum. Mol. Genet.* **26**, 1535–1551.

Rohrbach M., Clarke J. T. R. (2007) Treatment of lysosomal storage disorders : progress with enzyme replacement therapy. *Drugs* **67**, 2697–2716.

Sands M., Davidson B. (2006) Gene therapy for lysosomal storage diseases. *Mol. Ther.* **13**, 839–849.

Sands M. S., Haskins M. E. (2008) CNS-directed gene therapy for lysosomal storage diseases. *Acta Paediatr.* **97**, 22–27.

Saraiva J., Nobre R. J., Pereira de Almeida L. (2016) Gene therapy for the CNS using AAVs: The impact of systemic delivery by AAV9. *J. Control. Release* **241**, 94–109.

Simonato M., Bennett J., Boulis N. M., Castro M. G., Fink D. J., Goins W. F., Gray S. J., et al. (2013) Progress in gene therapy for neurological disorders. *Nat. Rev. Neurol.* **9**, 277–291.

Siupka P., Hersom M. N., Lykke-Hartmann K., Johnsen K. B., Thomsen L. B., Andresen T. L., Moos T., Abbott N. J., Brodin B., Nielsen M. S. (2017) Bidirectional apical–basal traffic of the cation-independent mannose-6-phosphate receptor in brain endothelial cells. *J. Cereb. Blood Flow Metab.* **37**, 2598–2613.

Storch J., Xu Z. (2009) Niemann-Pick C2 (NPC2) and intracellular cholesterol trafficking. *Biochim. Biophys. Acta* **1791**, 671–8.

Tajes M., Ramos-Fernández E., Weng-Jiang X., Bosch-Morató M., Guivernau B., Eraso-Pichot A., Salvador B., Fernàndez-Busquets X., Roquer J., Muñoz F. J. (2014) The blood-brain barrier: Structure, function and therapeutic approaches to cross it. *Mol. Membr. Biol.* **31**, 152–167.

Takahashi K., Yamanaka S. (2006) Induction of Pluripotent Stem Cells from Mouse Embryonic and Adult Fibroblast Cultures by Defined Factors. *Cell* **126**, 663–676.

Thomsen L. B., Burkhart A., Moos T. (2015) A Triple Culture Model of the Blood-Brain Barrier Using Porcine Brain Endothelial cells, Astrocytes and Pericytes. *PLoS One* **10**, 1–16.

Thomsen L. B., Lichota J., Kim K. S., Moos T. (2011) Gene delivery by pullulan derivatives in brain capillary endothelial cells for protein secretion. *J. Control. Release* **151**, 45–50.

Thomsen M. S., Birkelund S., Burkhart A., Stensballe A., Moos T. (2017) Synthesis and deposition of basement membrane proteins by primary brain capillary endothelial cells in a murine model of the blood-brain barrier. *J. Neurochem.* **140**, 741–754.

Vanier M., Millat G. (2003) Niemann-Pick disease type C. *Clin. Genet.* **64**, 269–281.

Vanier M. T. (2010) Niemann-Pick disease type C. *Orphanet J. Rare Dis.* **5**, 1–18.

Vanier M. T., Millat G. (2004) Structure and function of the NPC2 protein. *Biochim. Biophys. Acta* **1685**, 14–21.

Vatine G. D., Al-Ahmad A., Barriga B. K., Svendsen S., Salim A., Garcia L., Garcia V. J., et al. (2017) Modeling Psychomotor Retardation using iPSCs from MCT8-Deficient Patients Indicates a Prominent Role for the Blood-Brain Barrier. *Cell Stem Cell* **20**, 831–843.

Wraith J. E., Baumgartner M. R., Bembi B., Covanis A., Levade T., Mengel E., Pineda M., et al. (2009) Recommendations on the diagnosis and management of Niemann-Pick disease type C. *Mol. Genet. Metab.* **98**, 152–165.

Yu J., Vodyanik M. A., Smuga-Otto K., Antosiewicz-Bourget J., Frane J. L., Tian S., Nie J., et al. (2007) Induced pluripotent stem cell lines derived from human somatic cells. *Science (80-.).* **318**, 1917–1920.

FIGURE LEGENDS

Figure 1. Characterization of human skin fibroblasts. a) Human skin fibroblasts from healthy (WT) and a Niemann Picks type C2 disease patient (NPC2 deficient) were characterized based on their expression of the fibroblast marker vimentin and filipin III. Filipin III binds specifically to cholesterol and is, therefore, a direct measure of the amount of cholesterol inside the lysosomes. Wildtype (WT) fibroblasts are smaller than the NPC2 deficient fibroblasts, and only NPC2 deficient fibroblasts show high cholesterol accumulation around the nucleus, probably corresponding to the site of the lysosomes. The cholesterol load in the NPC2 deficient fibroblasts is corrected by the addition of 10µg/ml bovine NPC2 protein (bNPC2), which is taken up by the cells via the mannose-6-phosphate receptor (MPR300), expressed in both cell types. **b)** Nuclei are counterstained with Gelred (blue). Scale bar 20µm. **c)** Quantification of the cholesterol load based on the fluorescent intensity of filipin per cell reveals that WT fibroblasts have significantly lower cholesterol than the NPC2 deficient fibroblasts ($P<0.0001$). The addition of bNPC2 results in a significantly lower cholesterol load compared to untreated NPC2 deficient fibroblasts ($P=0.031$). No significant difference is observed between WT and bNPC2 treated fibroblasts ($P=0.0715$). Data are presented as mean ± SEM (n=8-10 images) and analyzed using a non-parametric Kruskal-Wallis t-test with Dunn's multiple comparison post hoc test. ***$P< 0.001$, *$P<0.05$, significantly different from untreated NPC2 deficient fibroblasts

Figure 2. Transfection of NPC2 deficient fibroblasts. NPC2 deficient fibroblasts were genetically modified to express NPC2 coupled to an orange fluorescent protein (OFP) to evaluate the functionally of the recombinant NPC2-OFP protein**.** The transfected NPC2 deficient fibroblasts were stained for vimentin (green), NPC2-OFP (red) and cholesterol (filipin III) (white). Only NPC2-OFP expressing fibroblasts are observed in the genetically modified fibroblasts. NPC2-OFP expressing fibroblasts reveal a decreased cholesterol load around the nucleus compared to that of the non-transfected NPC2 deficient fibroblasts, suggesting that recombinant NPC2-OFP is functional and able to reverse the accumulated cholesterol load in the NPC2 deficient fibroblasts. Scale bar 20µm

Figure 3. Transfection of primary rat brain capillary endothelial cells (rBCECs) in co-cultures with primary rat astrocytes. **a)** rBCECs were genetically modified to express recombinant NPC2 coupled to an orange fluorescent protein (OFP). NPC2-OFP expressing cells are only observed in the transfected rBCECs (red) and double labeling with an anti-NPC2 antibody (green) reveals co-localization between OFP and recombinant NPC2 (merged). **b)** The percentage of genetically modified cells expressing NPC2 is 7, which

were counted based on the fluorescent signal of the OFP using flow cytometry analysis, and found to be significantly higher than non-transfected cells (P=0.0025). Data are presented as mean ± SEM (n=5-7 samples (each pooled from 3 filters)) and analyzed using a non-parametric Mann-Whitney test. **P<0.01. **c)** Immunocytochemistry was performed to evaluate the protein expression of four important tight junction proteins (ZO1, ZO2, CLD5, and OCLN) (green). NPC2-OFP (red) expressing cells are observed only among the transfected cells. To evaluate a possible effect of transfection on the expression of the tight junction proteins, framed areas are shown in higher magnification. However, despite being genetically modified, they maintained a robust expression of tight junctions proteins, like those found in non-transfected cells. Nuclei are counterstained with DAPI (blue). Scale bar 20μm

Figure 4. Transfection influence on barrier integrity and permeability. a) The effect of transfection on co-cultured rat brain capillary endothelial cells' (rBCECs) ability to maintain barrier integrity was monitored using measurements of trans-endothelial electrical resistance (TEER) and compared to that of non-transfected cells. The rBCECs are initially induced to increase their expression of BBB characteristics (like increased tight junction expression) by the addition of CTP-cAMP, RO, HC, and astrocytes. 24 hours later the rBCECs display TEER values above 150 $\Omega*cm^2$, indicative of high barrier integrity, at which point transfection could be initiated for 24 hours. Data are presented as mean ± SEM (n=37-49 filters). **b)** The percentage difference in TEER values before and after transfection was calculated. The transfection did not affect the barrier integrity (P=0.2537). Data are presented as mean ± SEM (n=37-49 filters) and analyzed using a non-parametric Mann-Whitney test. **c+d)** The apparent permeability (Papp) to mannitol was used to assess the effect of transfection on the rBCECs permeability. The rBCECs were transfected for 24 hours, after which the Papp for mannitol was calculated. **c)** Papp for both non-transfected and transfected rBCECs were in the range of $4.0*10^{-6}$ and $1.0*10^{-6}$ cm/s with TEER values ranging from 270 to 477 $\Omega*cm^2$ (n=10 filters). **d)** No significant differences were found in the permeability to mannitol between non-transfected rBCECs and transfected BCECs (n=10 filters) (P=0.5579, df=20), indicating that transfection did not have any effect on the permeability. Data are presented as mean ± SEM (n=37-49 filters) and analyzed using a parametric unpaired t-test.

Figure 5. Secretion of NPC2 from rat brain endothelial cells (rBCECs) in co-cultures with primary astrocytes. a) Transport of NPC2 across the *in vitro* blood-brain barrier model was investigated by the addition of 5ng/ml NPC2 to either the upper or lower chamber and the media analyzed 24 hours later by ELISA. No transport of NPC2 was observed in either direction, but only approximately 30% of the added NPC2 was recovered, indicating a high uptake of NPC2 into the cells (rBCECs and astrocytes). Data are presented as mean ± SEM (n=8 filters). **b)** rBCECs were genetically modified for 24h, and the concentration of NPC2 in the media from both the upper and lower chamber was determined using ELISA. Transfected rBCECs secrete low amounts of NPC2 into the media, and mainly towards the upper chamber

(0.4 ng/ml in the upper chamber and 0.09ng/ml in the lower chamber). NPC2 secretion from transfected rBCECs was significantly increased compared to NPC2 secretion from non-transfected cells (P=0.0001 (upper), P=0.0011 (lower)) (statistical analysis was only performed between each corresponding chamber (upper vs upper, lower vs lower). Data are presented as mean ± SEM (n= 6-10 filters) and analyzed using a non-parametric Mann-Whitney test. ***P< 0.001, **P<0.01 **c)** The media from the upper and lower chambers were added to NPC2 deficient fibroblasts for 48 hours. Fibroblasts were identified based on vimentin staining (green). The amount of cholesterol was evaluated based on filipin III staining (white), and nuclei are counterstained with Gelred™. No clear differences are observed between the cholesterol load in fibroblasts treated with media from the upper and lower chambers of transfected and non-transfected cells. Scale bar 20µm. **d)** Quantification of the cholesterol load in fibroblasts after treatment was evaluated based on the cytochemical stainings. In spite, the significant secretion of NPC2 from rBCECs (b), the amount of NPC2 secreted from the transfected rBCECs is too low to correct the cholesterol load in the deficient fibroblast (P>0.88, df=37). Data are presented as mean ± SEM (n=9-11 images) and analyzed using a parametric one-way ANOVA with Tukey's multiple comparisons post hoc test.

Figure 6. Secretion of NPC2 from rat brain endothelial cells (rBCECs) in monocultures and HeLa cells. **a)** Mono-cultured rBCECs and HeLa cells were genetically modified to express and secrete recombinant NPC2, and stained using an anti-NPC2 antibody (red). rBCECs (mono) were additionally stained with the tight junction marker ZO1 (Green). Only NPC2 expressing cells is observed when the cells are transfected. Nuclei are counterstained with DAPI and reveal no mitotic cells among the rBCECs. Scale bar 20µm. **b)** The percentage of transfected rBCECs and HeLa cells in monocultures is 21 and 75, respectively (P=0.0028 (RBEC), and P=0.0011 (HeLa)). Data are presented as mean ± SEM (n=4-9 samples (each pooled from 3 filters)) and analyzed using a non-parametric Mann-Whitney test. **P<0.01. **c)** Opposed to the non-significant effects observed when cultured in co-cultures, the higher percentage of transfected rBCECs in monocultures resulted in a higher concentration of secreted NPC2 (3.3ng/ml) (P<0.0001) compared with Fig. 5. The concentration of NPC2 secreted from HeLa cells was even higher (16 ng/ml) (P<0.0001). Non-transfected cells do not secrete NPC2. Data are presented as mean ± SEM (n=8-11 filters) and analyzed using a non-parametric Mann-Whitney test, ***P<0.001. **d)** Fibroblasts were identified with an anti-vimentin antibody (green) and the nuclei counterstained with Gelred™ (blue). The cholesterol load was identified using filipin III (white). Treatment of NPC2 deficient fibroblasts with media from transfected rBCECs (mono) and HeLa cells results in partial and widespread correction of the cholesterol load, respectively, compared to NPC2 deficient fibroblasts treated with media from non-transfected cells. Scale bar 20µm. **e)** Quantification of the cholesterol load in the treated fibroblasts reveals a significant correction of cholesterol load in the fibroblasts treated with media from transfected rBCECs

compared to fibroblasts treated with non-transfected media (P=0.0344, df=19). Examination of fibroblasts treated with media from transfected HeLa cells reveals a complete correction to the same extent as that seen in Wild type (WT) fibroblasts (Fig. 1c) (P<0.0001). Data are presented as mean ± SEM (n=10-11 images) and analyzed using a parametric unpaired t-test (RBEC) and a non-parametric Mann-Whitney test (HeLa). ***P<0.001, *P<0.05

Figure 7. A hypothetical model for genetically modifying the brain capillary endothelial cells (BCECs) to secrete recombinant NPC2 as a strategy to treat Niemann Picks type C2 Disease. A vector coupled to genetic material (e.g. a plasmid) encoding Niemann Picks type C2 protein (NPC2) will be taken up by the BCECs and undergo endocytosis and endosomal escape to avoid degradation in the lysosomal system. The genetic material will enter the cell nucleus where it will be transcribed to mRNA, transported out of the nucleus and translated to proteins. NPC2 will either be carried to the genetically modified cells' endosomal system or be packaged in vesicles for secretion. This secretion can be bi-directional meaning the protein will be released either in the direction of the blood or into the brain parenchyma. NPC2 deficient cells do not have a functional NPC2 protein and therefore do not have a functional clearance of cholesterol from their late-endosomal lysosomal system. Normally cholesterol is taken up by the cells via the low-density lipoprotein (LDL) receptor in the form of LDL. Inside the endosomes, LDL becomes hydrolyzed to cholesterol. NPC2 present in the endosomes will bind cholesterol, and, via an interplay with NPC1, facilitate the transport of cholesterol out of the endosomes to the Golgi apparatus, the cell membrane or via the release as high-density lipoprotein (HDL). When NPC2 expression is non-functional, cholesterol will build up inside the lysosomes. NPC2 secreted from the genetically modified BCECs can be taken up by NPC2 deficient cells via the mannose-6-phosphate receptor (MPR300), which will carry NPC2 to the endosomes where it will bind to cholesterol and restore cholesterol transport. Since the secretion of NPC2 from genetically modified BCECs is bi-directional the strategy will theoretically supply NPC2 to NPC2 deficient cells both within and outside of the central nervous system. *Abbreviations: A, Astrocytes; E, Endothelial cells; EE, Early endosomes; ER, Endoplasmatic reticulum; LE, Late endosome; N, Neuron; P, Pericyte*

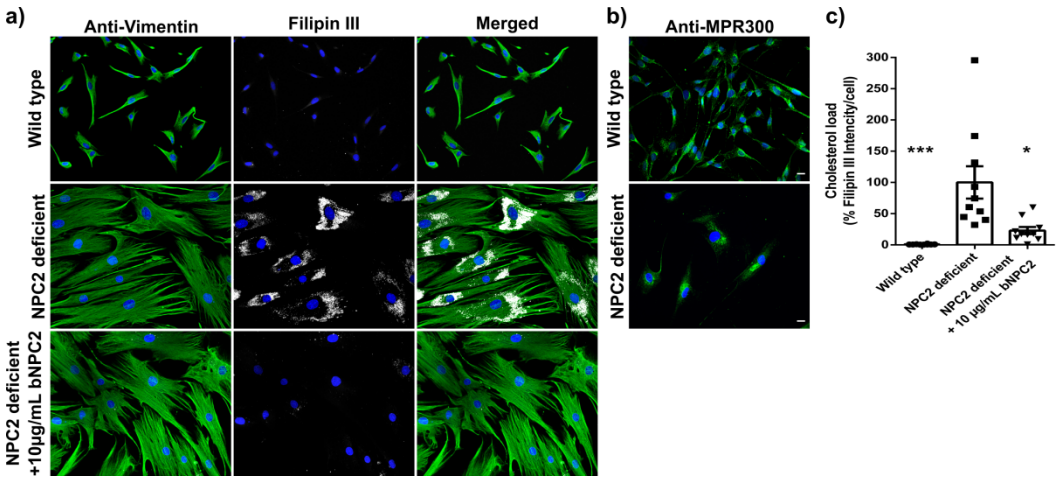

jnc_14982_f1.tif

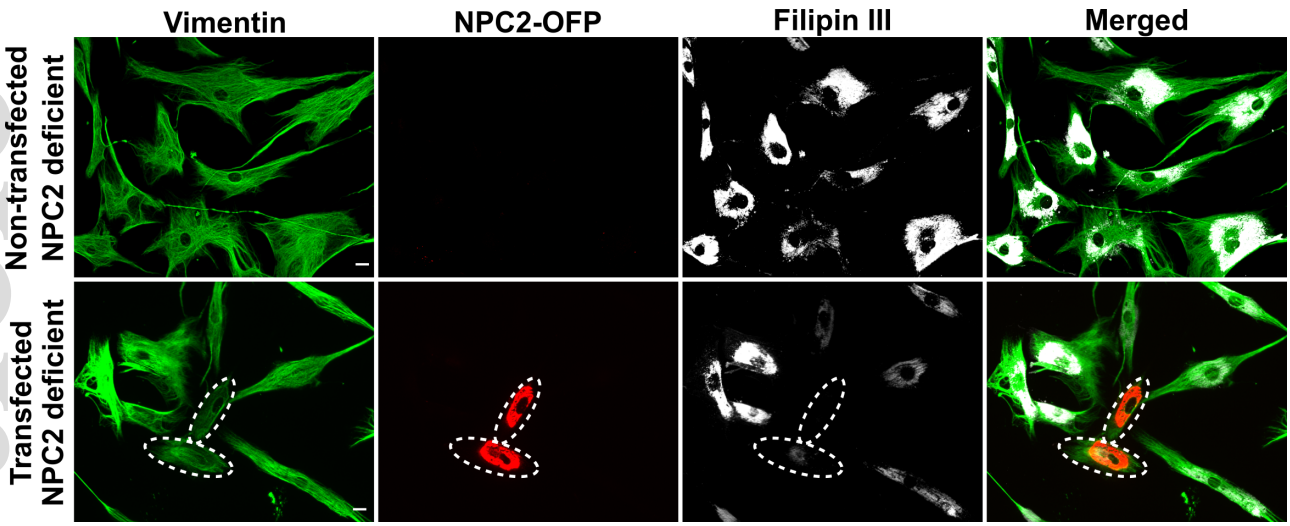

jnc_14982_f2.tif

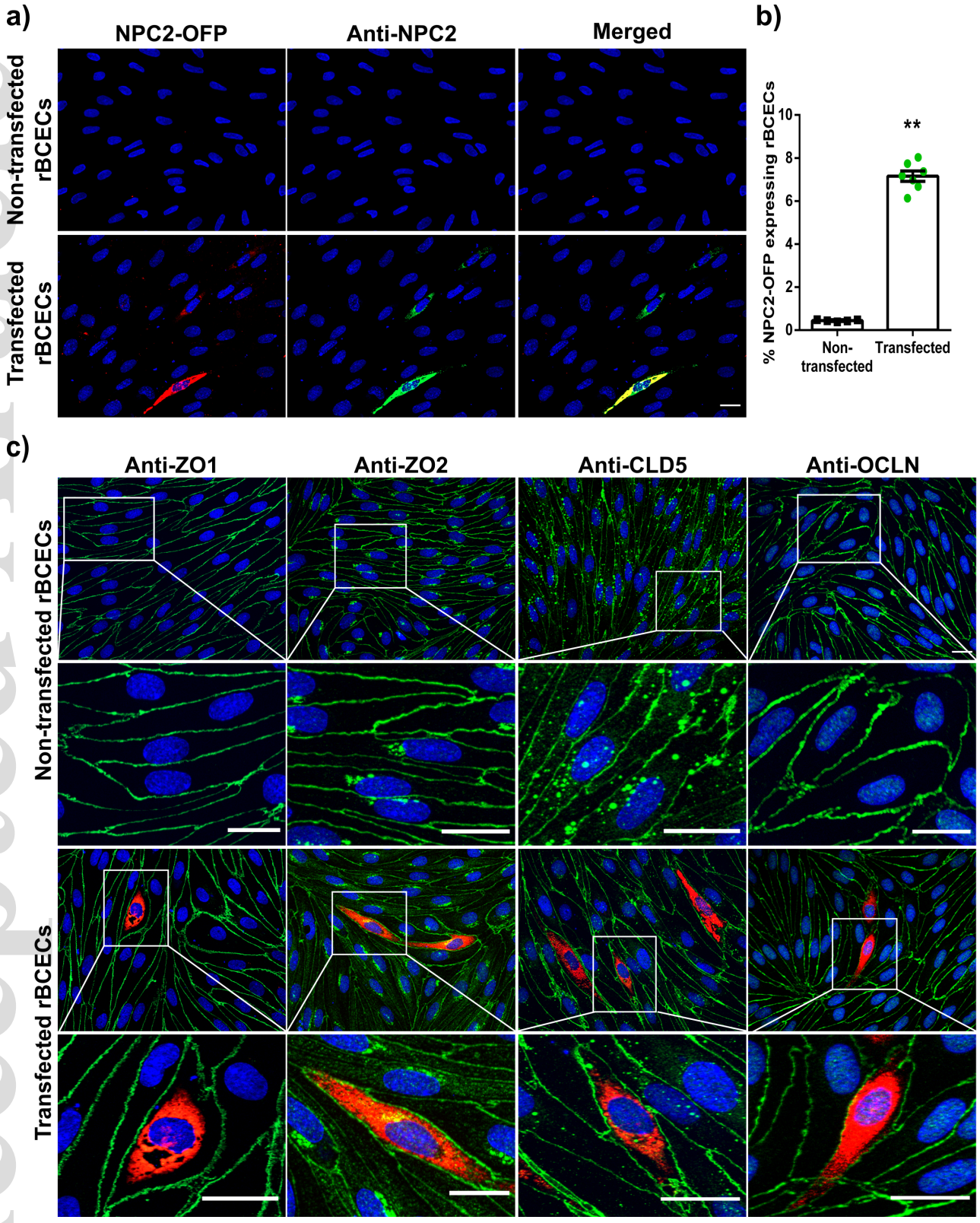

jnc_14982_f3.tif

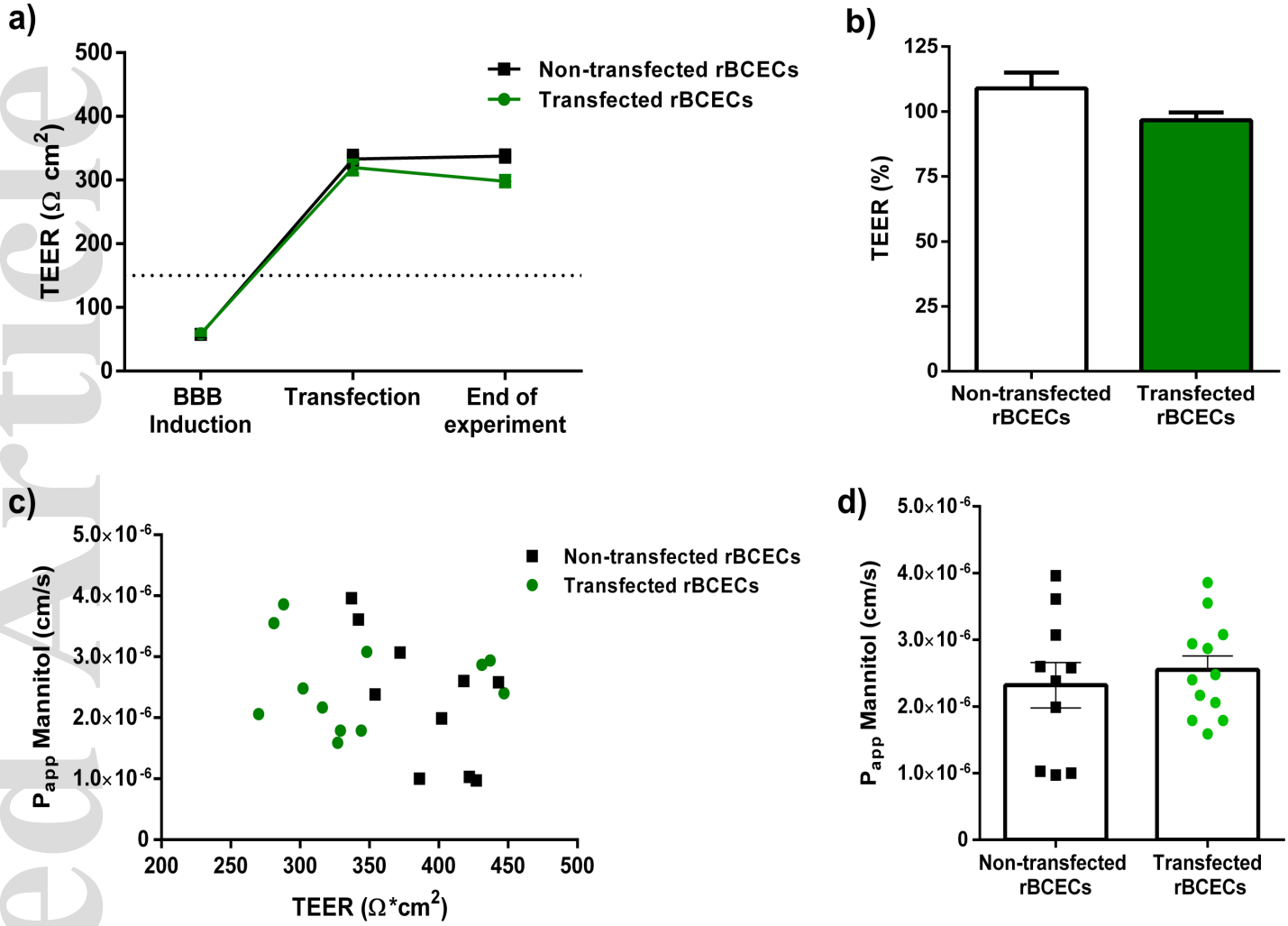

jnc_14982_f4.tif

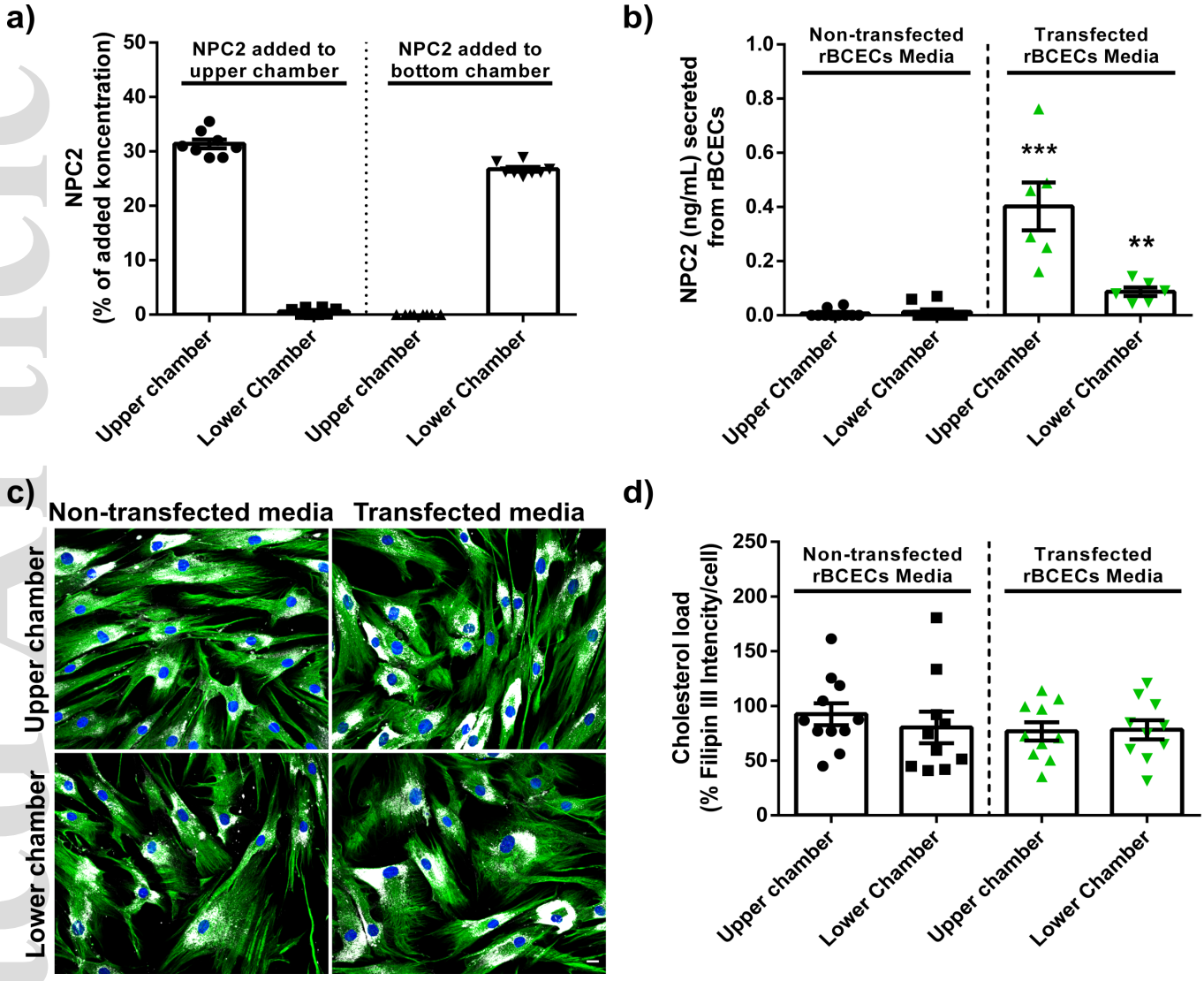

jnc_14982_f5.tif

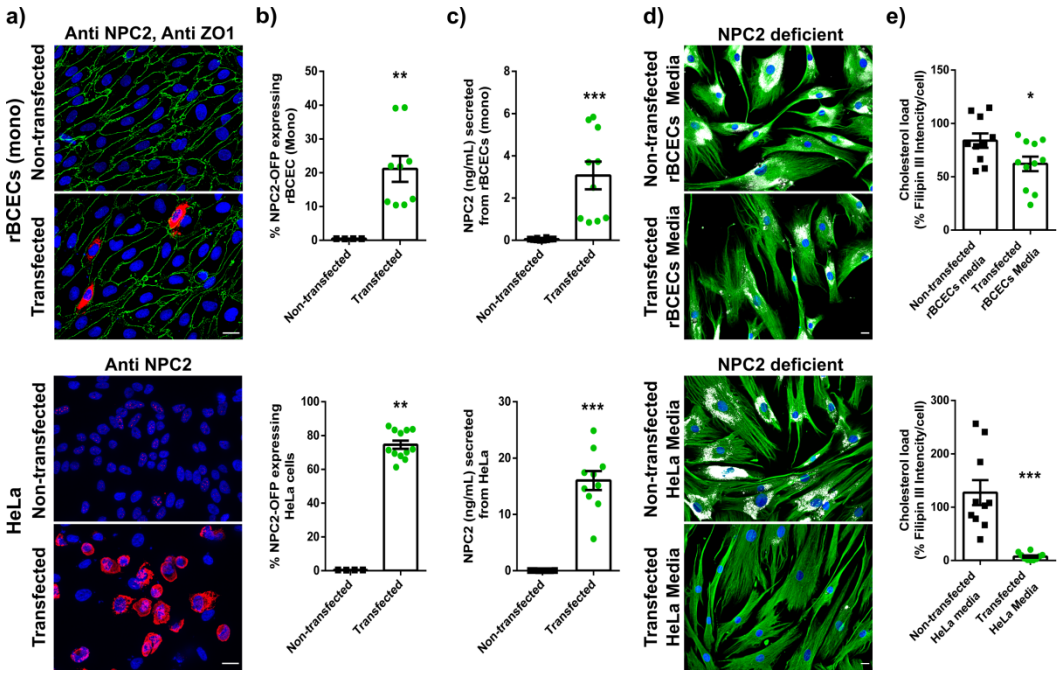

jnc_14982_f6.tif

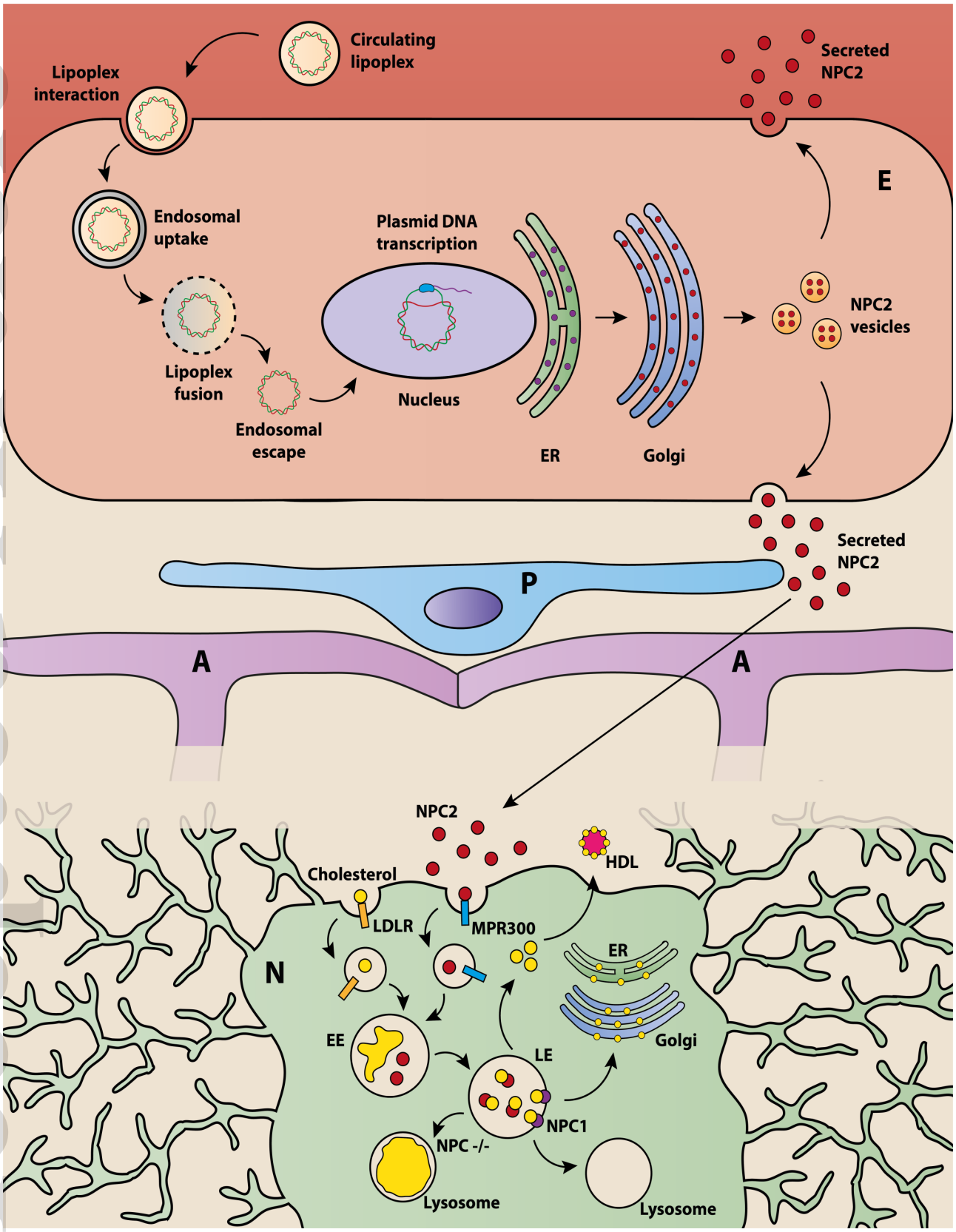

jnc_14982_f7.tif